Supporting Information

Photothermal Effect Enables Markedly Enhanced Oxygen Reduction and Evolution Activities for High-Performance Zn–Air Batteries

Xiaoyan Zhang,[a] Shuang Pan,[a] Huanhuan Song,[a] Wengai Guo,[a] Fan Gu,[a] Chengzhan Yan,[a] Huile Jin,[a] Lijie Zhang,[a] Yihuang Chen,[a] and Shun Wang,*[a]*

[a]College of Chemistry and Materials Engineering, Institute of New Materials and Industrial Technologies, Wenzhou University, Wenzhou 325035, PR China
E-mail: yhchen@wzu.edu.cn; shunwang@wzu.edu.cn

1. Experimental Section

1.1 Materials Synthesis

Synthesis of Graphene Oxide (GO)

GO was prepared via a modified Hummers method.[1,2] Typically, 1g of graphite (99%+) was added into a 250 ml round-bottom flask, followed by adding 25 ml of 98% sulfuric acid. Then, the solution was stirred for 24 h at room temperature. Subsequently, 200 mg of $KMnO_4$ was slowly added into the mixture solution and stirred for 5 min until 1g of $KMnO_4$ was added. Meanwhile, the solution was kept under stirring for 30 min. Afterwards, 46 ml of deionized water (DIW) was added to the mixture drop by drop at the same time. After that, 140 ml of DIW and 10 ml of 30% H_2O_2 were added to the mixture and stirred for 5 min. A vacuum was then pumped to remove the solution. The obtained was washed with 180 ml of 5% HCl solution and enough DIW until the solution was neutral. After being washed with anhydrous ethanol, the obtained suspension was sonicated for 1 h followed by centrifugation at 3000 rpm for 5 min, yielding the final product.

Synthesis of Co_3O_4/N-rGO

To prepare Co_3O_4/N-rGO, 8 mg of GO was dispersed in 24 ml of anhydrous ethanol with ultrasonication for 12h. Subsequently, 48 mg of cobalt acetylacetonate ($Co(Ac)_2$), 0.5ml of ammonia water and 0.7 mL of DIW were added to the GO ethanol solution with ultrasonication for 30 min. The mixture solution was then stirred at 80°C for 10 h and transferred into a 50 mL stain steel autoclave at 150 °C for 3 h. The obtained suspension was sonicated for 30 min followed by centrifugation and washing with anhydrous ethanol and DIW for 3 times, yielding the final product.

Synthesis of Co_3O_4/rGO, N-rGO, and Co_3O_4 nanoparticles.

To prepare Co_3O_4/rGO hybrid without the addition of NH_4OH, the first step reaction mixture was prepared by adding 48 mg of $Co(Ac)_2$ and 1.2 ml of DIW to 24 ml of GO anhydrous ethanol suspension with ultrasonication for 30 min. The following steps were the same as those for the synthesis of Co_3O_4/N-rGO. The resultant Co_3O_4/rGO was dried, grounded and collected.

N-rGO was synthesized by the thermal reduction of mixed powders containing GO and ammonia water. 8 mg of GO and 0.5 ml of ammonia water were dispersed in 24 ml of ethanol by ultrasonication for 30 min. The obtained solution was kept stirring at 80°C for 10 h and transferred into a 50 mL stain steel autoclave at 150 °C for 3 h. The following steps were the same as those for the synthesis of Co_3O_4/N-rGO.

Co_3O_4 nanoparticles were prepared through the same steps as those for Co_3O_4/N-rGO except the addition of GO.

1.2 Characterization

The morphology of GO and Co_3O_4/N-rGO was recorded by a field emission transmission electron microscopy (TEM) and High-Resolution transmission electron microscopy (HRTEM) on a JEOL 2100F instrument (operated at 200 kV). The crystalline structure of samples was obtained by XRD (Bruker D8 advanced). XRD samples were prepared by drop-casting their aqueous suspensions onto glass substrates. Thermal gravimetric analysis (TGA, Netzsch STA 449 f3) was utilized to measure the content of the hybrid nanosheets at a rate of 5°C min^{-1} from 25 to 800 °C in air. The surface area and the porosity distribution of the samples were investigated via Brunauer-Emmett-Teller analysis. The elements and electronic status of the samples were determined via X-

ray photoelectron spectroscopy (XPS) measurements on SES 2002 at a power of 120W (8 Ma, 15 kV).

1.3 Electrochemical Measurements

Cyclic voltammetry (CV)

All electrochemical tests were conducted in the three-electrode cell using CHI760D electrochemical analyzer at room temperature. Rotary disk electrode (RDE) coated with catalysts, Ag/AgCl (3 M KCl) or Hg/HgO (1 M KOH) electrode and graphite rod were used as the working electrode, reference electrode and counter electrode, respectively. O_2-saturated 0.1 M KOH and O_2-saturated 1 M KOH served as the electrolytes for ORR and OER, respectively. In all measurements, the data was *iR* corrected and the Ag/AgCl or Hg/HgO was calibrated with respect to reversible hydrogen electrode (RHE). The measured potential of the Ag/AgCl electrode was converted to the potential versus to the reversible hydrogen electrode (RHE) based on $E_{RHE} = E_{Ag/AgCl} + 0.21 + 0.0591$ pH-*iR*. The measured potential of the Hg/HgO electrode was converted to the potential versus to the reversible hydrogen electrode (RHE) based on $E_{RHE} = E_{Hg/HgO} + 0.098 + 0.0591$ pH-*iR*.

Rotating disk electrode (RDE) measurement

The catalyst ink was prepared by dispersing 6 mg of the as-prepared catalyst with 12 μL of Nafion, 200 μL of ethanol, and 800 μL of DIW in an ultrasonic bath for 1 h, and then 20 μL of the dispersion (containing 0.118 mg catalyst) was transferred onto a glassy carbon electrode of 5 mm in diameter (loading amount: 0.60 mg cm^{-2}). The as-prepared catalyst film was dried at room temperature. The scanning range of the OER system is 0 V ~ 1.0 V (vs. Hg/HgO). The scanning range of the ORR system is -1.0 V ~ 0 V (vs. Ag/AgCl), under various rotating speeds (400 rpm, 625 rpm, 900 rpm, 1225 rpm, 1600 rpm, 2025 rpm), and the scanning rate is 5 mV s^{-1}. The transferred electron number (n) in ORR was calculated from the slope of Koutecky-Levich (K-L) plot as follows.

$$(1)\ J^{-1}=J_L^{-1}+J_K^{-1}=(B\omega^{1/2})^{-1}+J_K^{-1},$$

$$(2)\ B=0.2nFC_0(D_0)^{2/3}v^{-1/6}$$

$$(3)\ J_K=nFkC_0$$

where J is the measured current density, J_K is the kinetic current density, ω is the rotation speed, n is the number of electron transfers, A is the effective area of the glassy carbon electrode, and F is Faraday Constant (F = 96485 C mol^{-1}), v is the kinetic viscosity (1.1×10^{-2} cm^2 s^{-1}), C_0 is the saturated concentration of oxygen in a 0.1 M KOH solution (1.2×10^{-3} mol L^{-1}), and D_0 is the diffusion coefficient of oxygen in a 0.1 M KOH solution (1.9×10^{-5} cm^2 s^{-1}). According to the above equation, the relation between J and ω can be obtained, and then the number of transferred electrons can be calculated. The EIS spectra of Co_3O_4/N-rGO were obtained at -0.2 V vs. Ag/AgCl and the frequency range varied from 0.01 to 100 kHz with 5 mV amplitude

Rotating ring-disk electrode (RRDE) measurement

RRDE measurement was carried out at the scan rate of 5 mV s^{-1} under the 1,600 rpm rotating speed. The scan range is from 0 ~ -1 V (vs. Ag/AgCl), and the ring potential is 1.5 V (vs. RHE). The following equations were used to calculate the percentage of H_2O_2 and the transferred electron number (n).

$$\%\,HO_2^- = 200 \times \frac{I_r/N}{I_d + I_r/N}$$

$$n = 4 \times \frac{I_r}{I_d + I_r/N}$$

where I_d is disk current, I_r is ring current and N is current collection efficiency of the Pt ring which was determined to be 0.40 from the reduction of $K_3Fe[CN]_6$.

To compare the performance, commercial 20 wt% Pt/C and RuO_2 catalysts were also studied, which prepared via same method and loading capacity.

Photothermal experiment

To scrutinize the photothermal-assisted performance, catalyst electrodes were irradiated with the 808 nm laser (MDL-H-808-5W) using a quartz reactor containing 0.1 or 1 M KOH solution. The temperature of the electrodes was tracked via an IR thermal camera (FLIR E50) until the electrode reached a steady temperature. As the electrode was immersed in electrolyte, there was a small temperature rise for the electrolyte near the surface of polytetrafluoroethylene (PTFE) due to the heat transfer between the electrode and its surrounding electrolyte, while the temperature of the rest of the electrolyte (i.e., major part) was almost unchanged. The temperature of the rest of the electrolyte was recorded as the temperature of the electrolyte. The reactor was put in a thermostatic water bath circulator, which guaranteed the temperature of electrolyte stay at room temperature. The irradiation power can be tuned in the range of 0–5.0 W cm^{-2}.

The fabrication and performance evaluation of the liquid rechargeable zinc–air batteries (ZABs)

The ZAB was fabricated using zinc foil and Co_3O_4/N-rGO loaded carbon fiber paper as the anode and air electrode, respectively. When performing the ZAB measurement, a rectangle-shape of zinc (0.5 cm * 0.8 cm) was cut and removed on zinc anode, forming a rectangle hole on the zinc foil (**Fig. 5a**). As such, the light, which came in from the direction of anode, was able to pass the zinc anode through the rectangle hole on the zinc foil and reached the air cathode side. 6 M KOH solution containing 0.2 M $Zn(Ac)_2$ severed as the electrolyte to ensure the reversible redox reaction of Zn anode. The catalyst loading on air electrode was 1.0 mg cm^{-2}. The charge-discharge recyclability performance was recorded at a constant current density of 10 mA cm^{-2} and 20 min for a cycle. For photothermal-assisted ZAB, prior to the battery testing, the ZAB was illuminated for 3 min to reach temperature equilibrium, followed by recording the performance of the battery.

All the ZABs were investigated under ambient atmosphere. The polarization curve measurements were performed by LSV (5 mV s^{-1}) at 25 °C with CHI760e electrochemical working station (CH Instrument). Both the current density and power density were normalized to the effective surface area of air electrode. The specific capacity was calculated according the equations below:

$$\frac{current * service\ hours}{weight\ of\ consumed\ zinc}$$

The energy density was calculated according the equation below:

$$\frac{current * service\ hours * average\ discharge\ voltage}{weight\ of\ consumed\ zinc}$$

2. Supplementary Figures and Tables

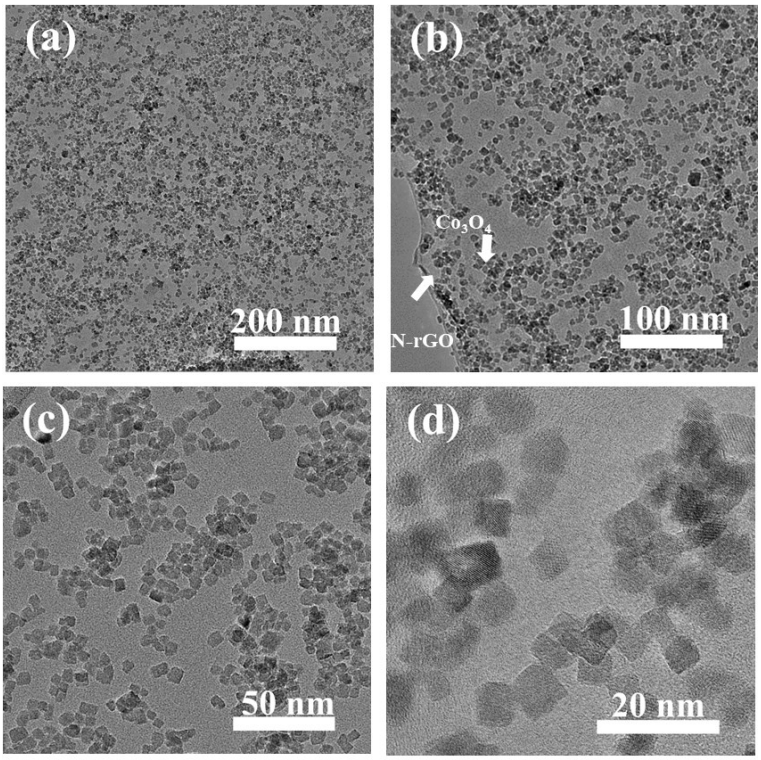

Supplementary Fig. 1 TEM images of Co_3O_4/N-rGO with different magnifications.

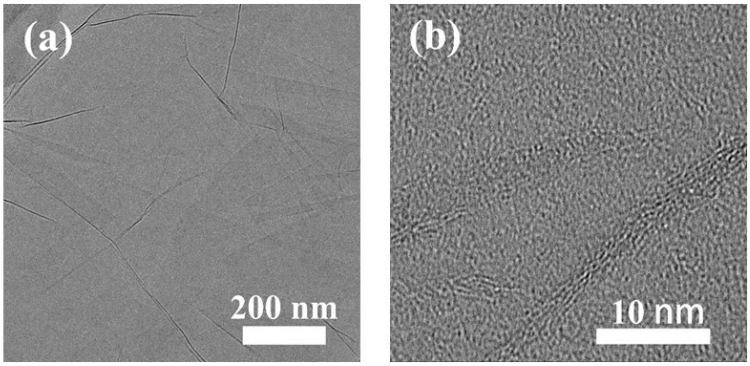

Supplementary Fig. 2 TEM images of GO with (a) low and (b) high magnifications.

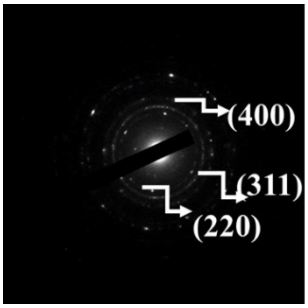

Supplementary Fig. 3 SAED patterns of Co_3O_4/N-rGO

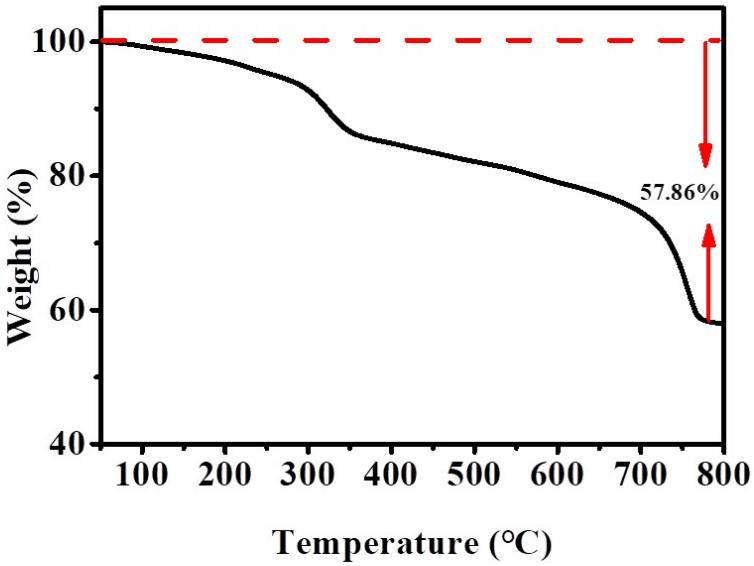

Supplementary Fig. 4 TGA curve of as-prepared Co_3O_4/N-rGO.

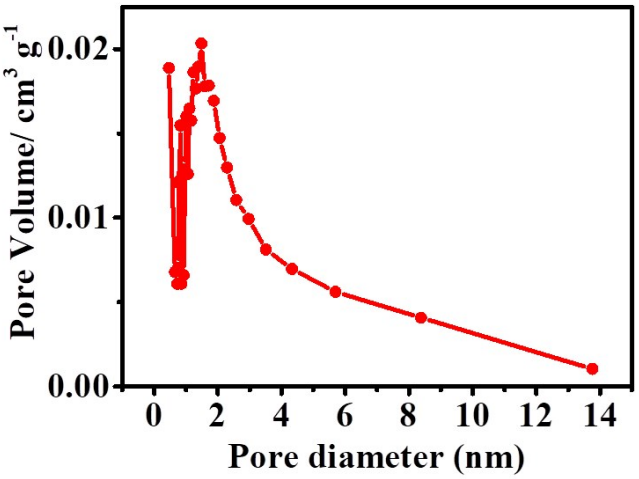

Supplementary Fig. 5 Pore size distribution of Co_3O_4/N-rGO.

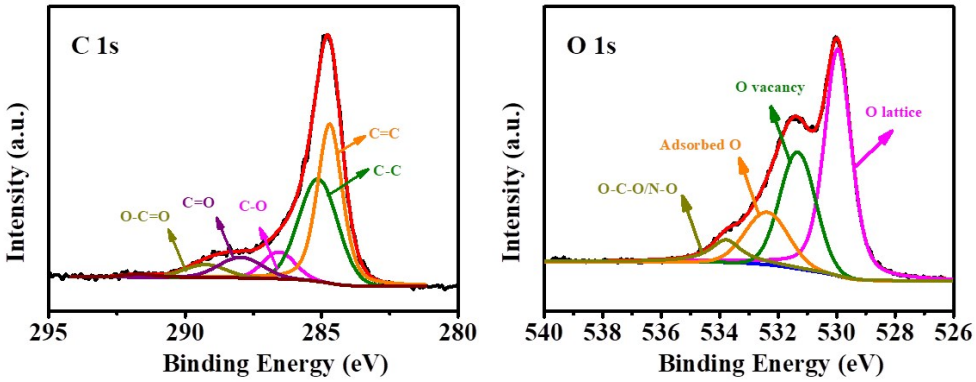

Supplementary Fig. 6 XPS spectra (C 1s and O 1s) of the as-synthesized Co_3O_4/N-rGO.

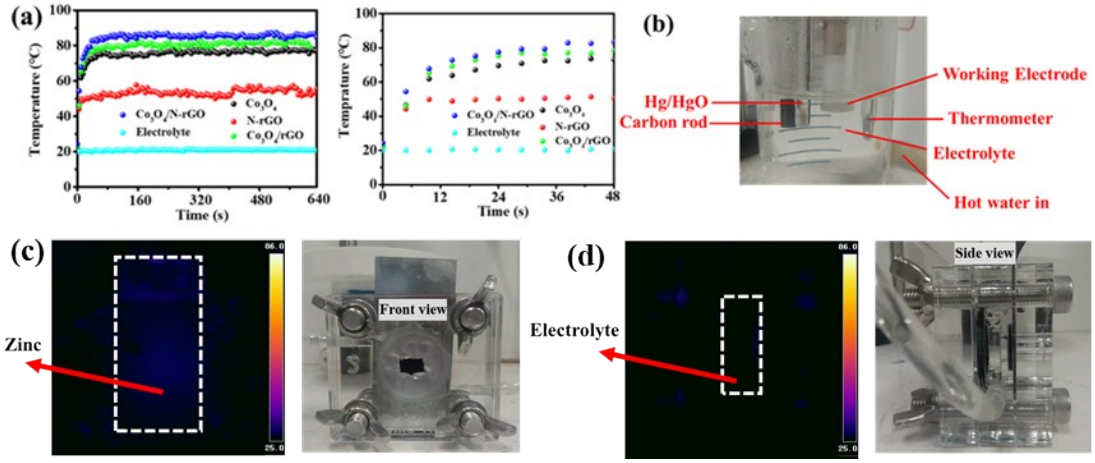

Supplementary Fig. 7 (a) Temperature variation over time (left) and enlarged range (right) of varied materials and electrolyte solution under 808 nm NIR irradiation. (b) Control experiment using circulating hot water rather than NIR light as the heating source. The obtained temperature was 65 °C for the whole setup including electrolyte, which underwent obvious evaporation during the heating and thus adversely influenced the performance of electrocatalysis and subsequent ZABs. Infrared images and corresponding digital images of (c) front and (d) side views during operation of ZAB at the presence of NIR light illumination. The increase of the test ambient temperature (i.e., heating the whole device) will not only lead to the increased temperature of air cathode (which is conducive to ZAB performance), but also result in adverse side-effects (e.g., leakage and evaporation of electrolyte, which restrict the improvement of ZAB performance) theoretically. In sharp contrast, our strategy enabled the localized heating of air cathode assisted by the photothermal effect, which did not affect the temperature of electrolyte or zinc anode and thus avoided the potential side-effects.

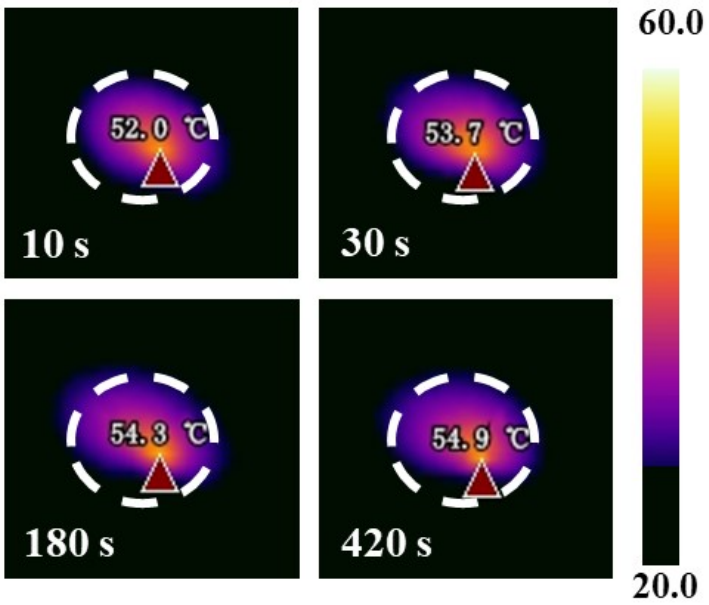

Supplementary Fig. 8 The temperature change over time (10 s, 30 s, 180 s, and 420 s) of Co_3O_4 electrode in 1M KOH electrolyte under 808 nm laser irradiation.

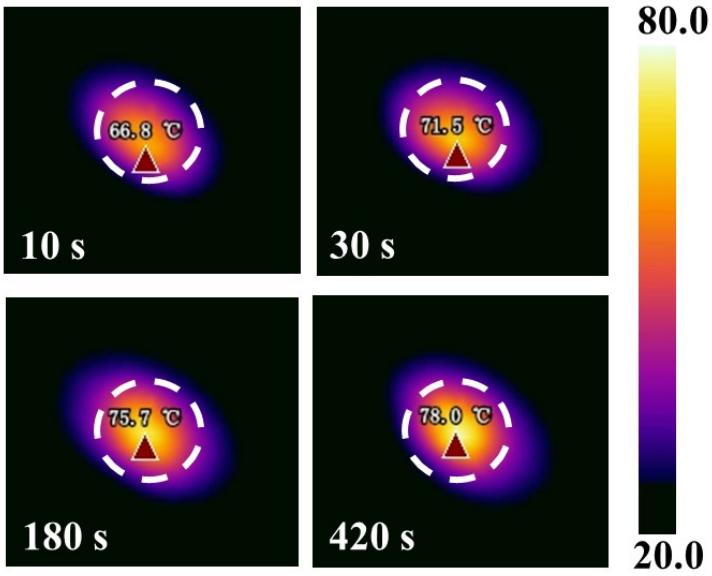

Supplementary Fig. 9 The temperature change over time (10 s, 30 s, 180 s, and 420 s) of N-rGO electrode in 1M KOH electrolyte under 808 nm laser irradiation.

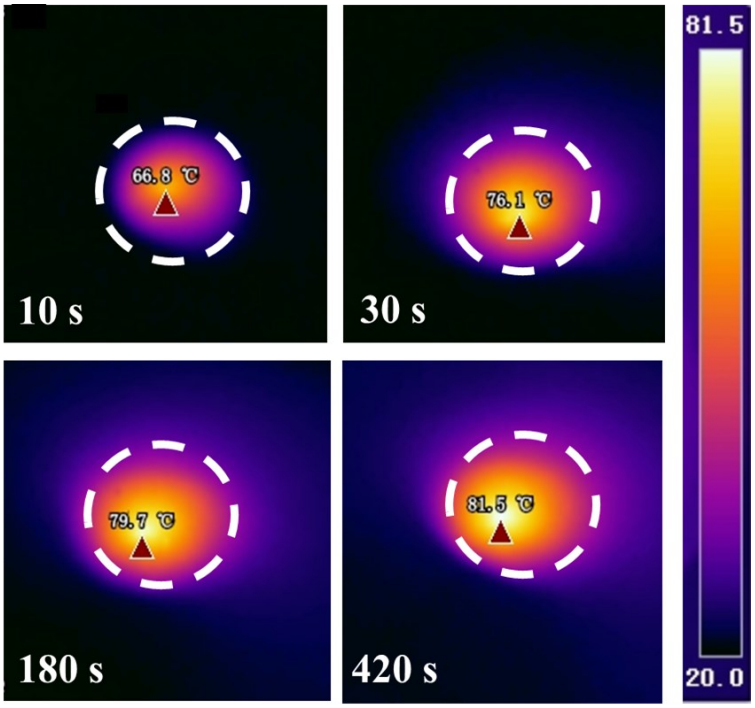

Supplementary Fig. 10 The temperature change over time (10 s, 30 s, 180 s, and 420 s) of Co_3O_4/rGO electrode in 1M KOH electrolyte under 808 nm laser irradiation.

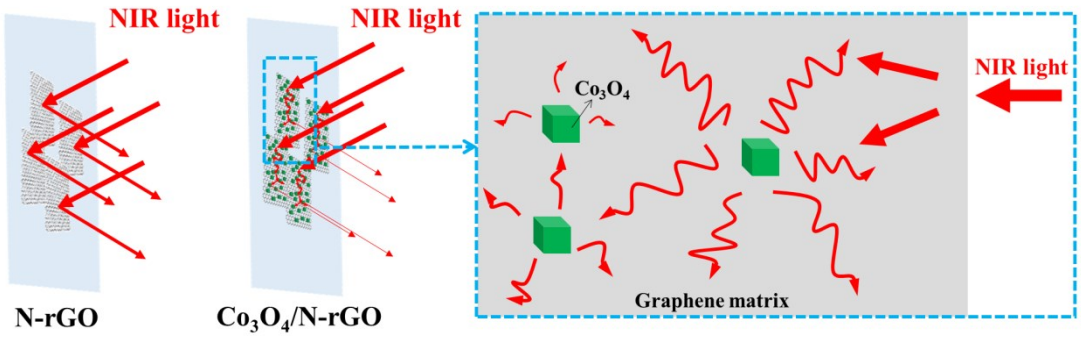

Supplementary Fig. 11 Schematic of light absorption for N-rGO (left) and Co_3O_4/N-rGO (right).

As the final temperature of Co_3O_4 (54.9℃) was lower than that of N-rGO (78℃) under NIR light irradiation, it is easy to understand that the modification of Co_3O_4 with N-rGO (i.e., Co_3O_4/ N-rGO) lead to a higher final temperature compared with pure Co_3O_4 due to the improved photothermal characteristic of materials. On the other hand, more light was scattered by the Co_3O_4 nanoparticles within the composite material (Co_3O_4/N-rGO) and the scattered light was absorbed by the graphene matrix (**Fig. S11**), leading to a significantly improved photo-to-thermal conversion compared with pure graphene. Similar observation was obtained in other work[3]. Therefore, the combination of graphene and Co_3O_4 as well as their synergy as an efficient light trapping medium resulted in the higher final temperature than that of single material (i.e., Co_3O_4 or N-rGO).

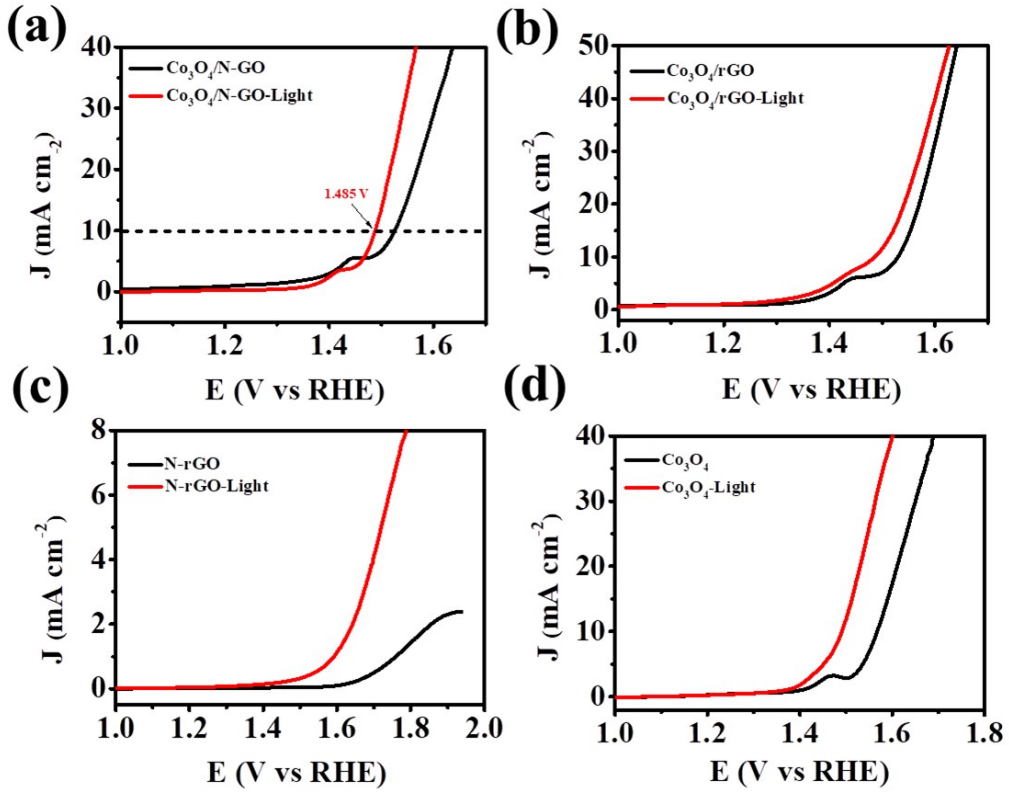

Supplementary Fig. 12 LSV polarization curves of (a) Co_3O_4/N-rGO, (b) Co_3O_4/rGO, (c) N-rGO, and (d) Co_3O_4 electrodes with or without light.

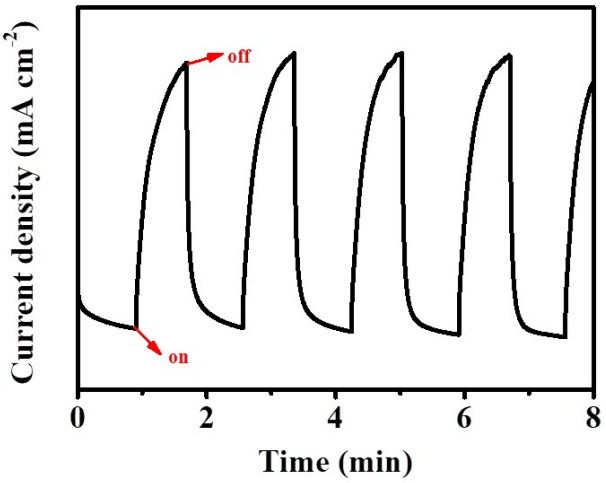

Supplementary Fig. 13 Current density over time of Co_3O_4/N-rGO electrode at a potential of 1.524 V_{RHE} under intermittent illumination.

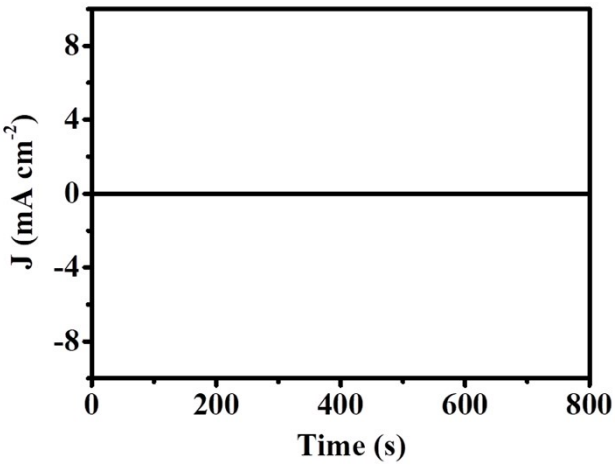

Supplementary Fig. 14 Photocurrent density for the Co_3O_4/N-rGO electrode with light.

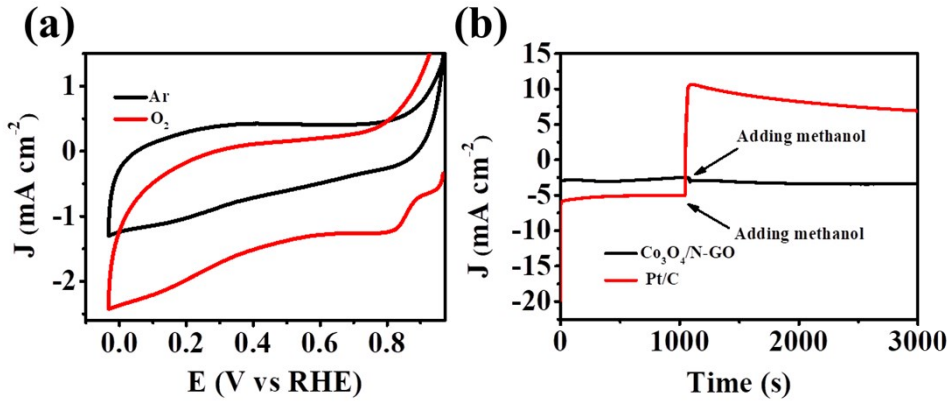

Supplementary Fig. 15 (a) CV of Co_3O_4/N-rGO in O_2/Ar-saturated solutions, all dates are measured at a scan rate of 5 mV/s. (b) Methanol resistance test of Co_3O_4/N-rGO and Pt/C.

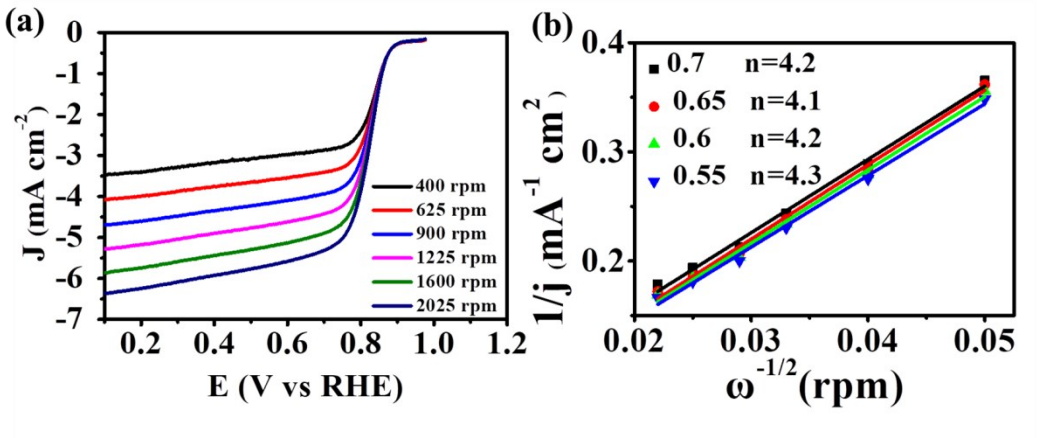

Supplementary Fig. 16 (a) ORR polarization curves of Co_3O_4/N-rGO at different rotating speeds. (b) The corresponding Koutecky-Levich plots at different potentials.

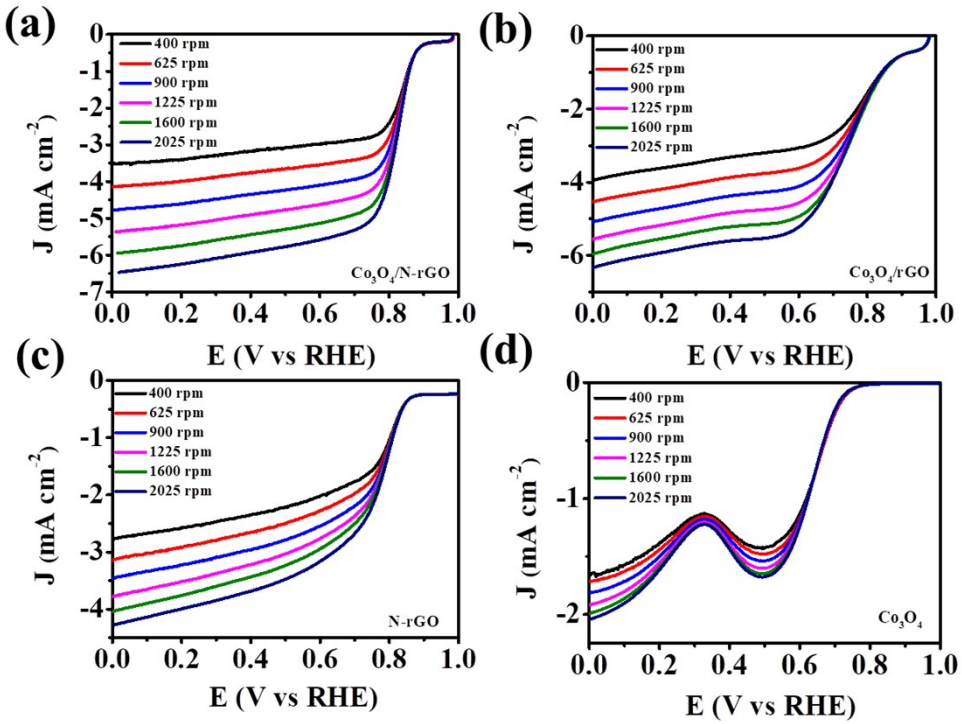

Supplementary Fig. 17 LSV curves of catalysts at different rotating speeds under O_2-saturated condition: (a) Co_3O_4/N-rGO (b) Co_3O_4/rGO, (c) N-rGO, and (d) Co_3O_4.

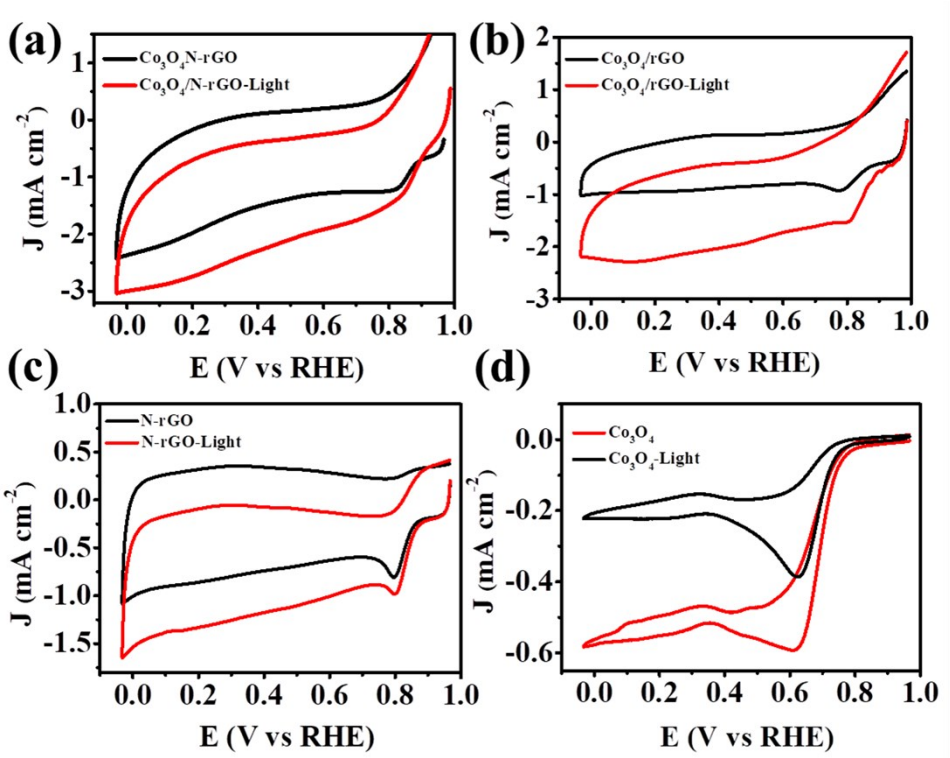

Supplementary Fig. 18 CV curves of catalysts in 0.1 M KOH O_2-saturated solution, all dates are measured at a scan rate of 5 mV/s: (a) Co_3O_4/N-rGO (b) Co_3O_4/rGO, (c) N-rGO, and (d) Co_3O_4 electrodes with or without light.

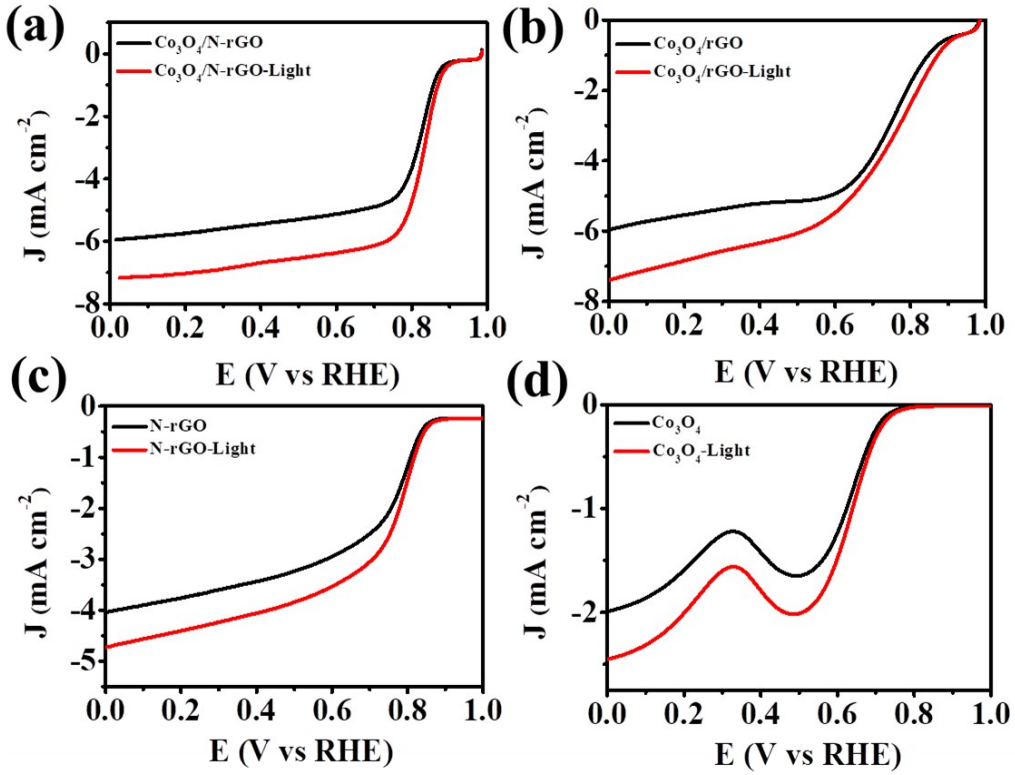

Supplementary Fig. 19 LSV polarization curves in ORR of (a) Co_3O_4/N-rGO, (b) Co_3O_4/rGO, (c) N-rGO, and (d) Co_3O_4 electrodes with or without light.

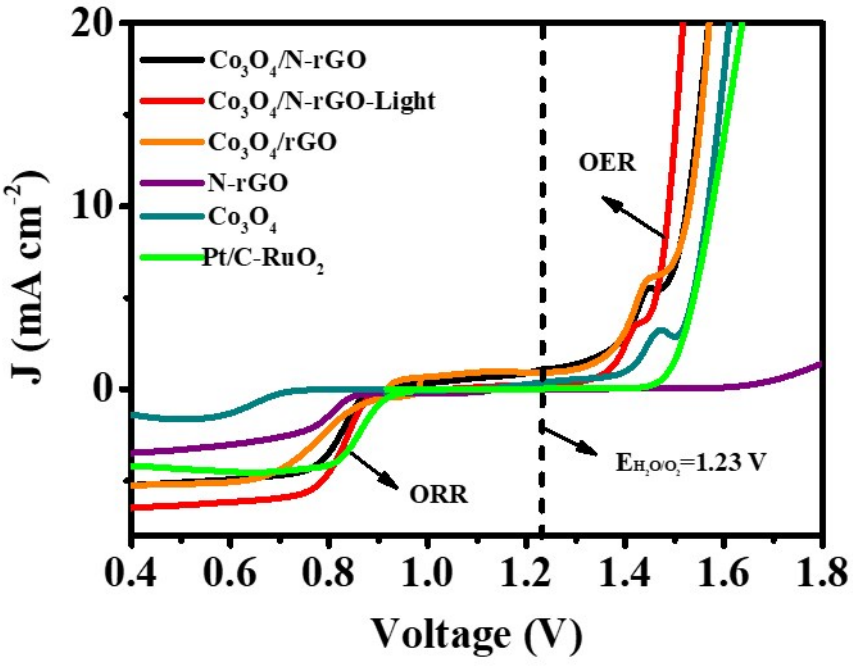

Supplementary Fig. 20 Bifunctional catalytic curves of Co_3O_4/N-rGO, Co_3O_4/rGO, Co_3O_4, N-rGO, RuO_2 and Pt/C.

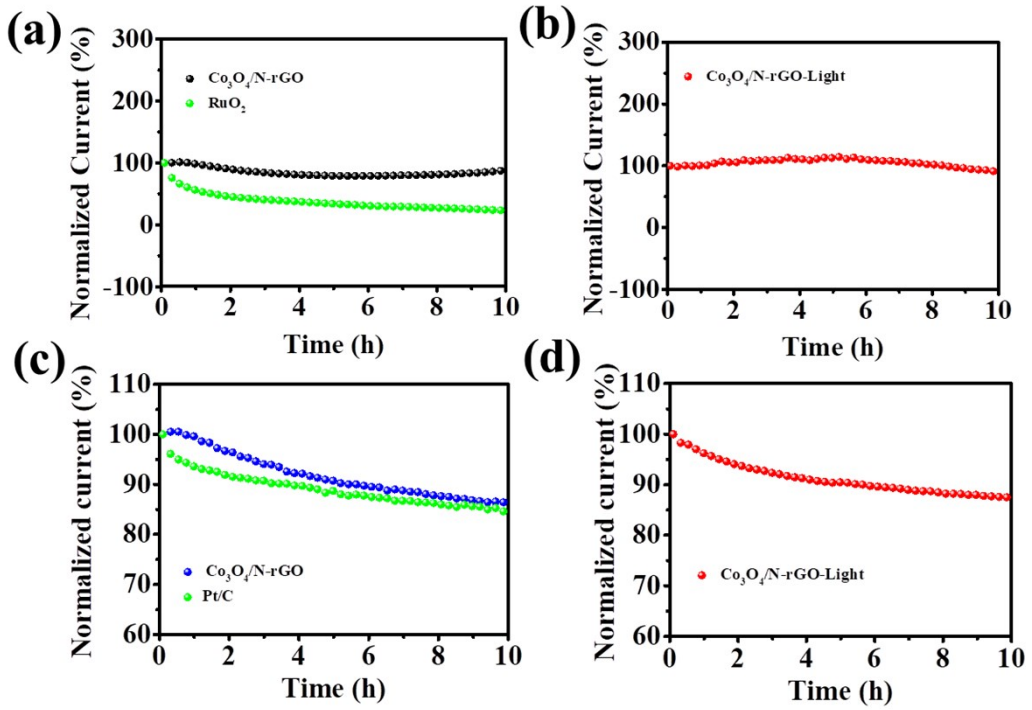

Supplementary Fig. 21 Stability test of catalysts in OER at a fixed current density of 10 mA cm^{-2} over 10 h: (a) Co_3O_4/N-rGO and commercial RuO_2 without light in 1 M KOH; (b) Co_3O_4/N-rGO with light in 1 M KOH. Stability test of catalysts in ORR at a fixed potential of 0.65 V_{RHE} over 10 h: (c) Co_3O_4/N-rGO and commercial Pt/C without light in 0.1 M KOH, (d) Co_3O_4/N-rGO with light in 0.1 M KOH.

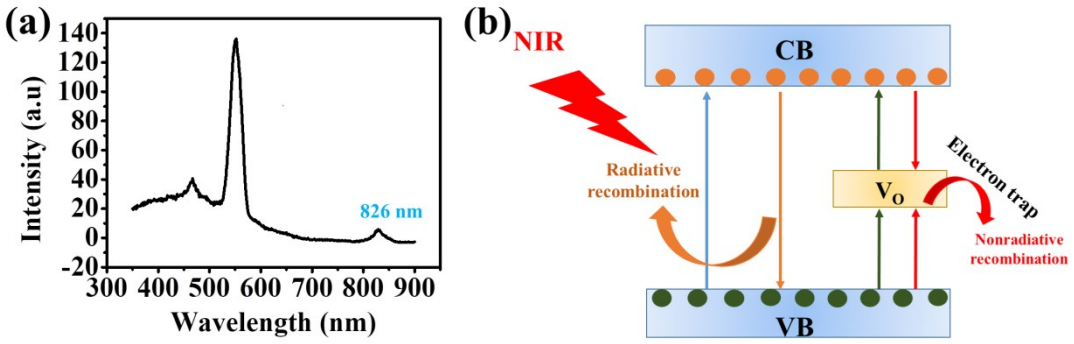

Supplementary Fig. 22 (a) Photoluminescence spectra of the Co_3O_4/N-rGO**.** (b) Schematic presentation for the photothermal effect of Co_3O_4.

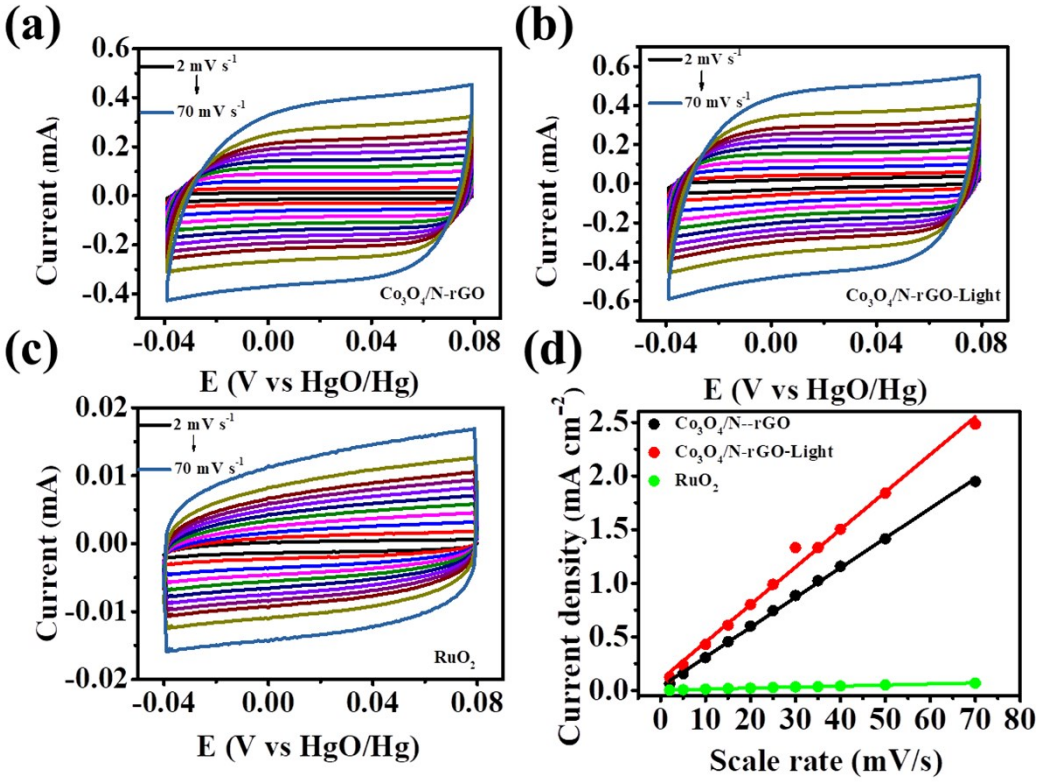

Supplementary Fig. 23 CV curves of electrodes with different scaning rate: (a) Co_3O_4/N-rGO without light, (b) Co_3O_4/N-rGO with light, (c) RuO_2 without light. (d) Corresponding double-layer capacitance (C_d) data derived from CV measurements at different scan rate.

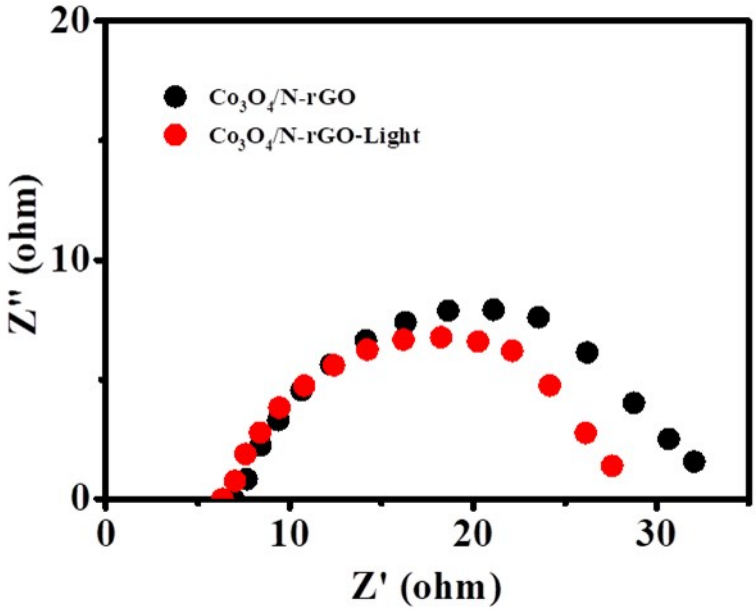

Supplementary Fig. 24 EIS response of Co_3O_4/N-rGO electrode in the absence and presence of NIR laser irradiation.

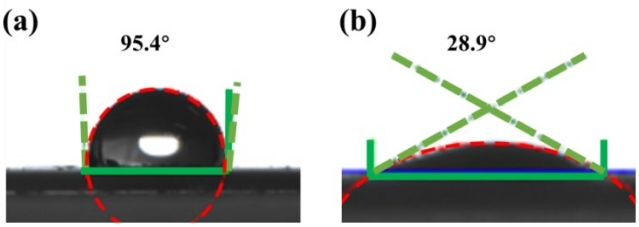

Supplementary Fig. 25 Contact angle images of the 1 M KOH on the Co_3O_4/N-rGO electrode surface (a) without and (b) with NIR light irradiation.

It is noteworthy that the fast release of as-formed O_2 bubbles is an crucial factor in OER process, since the adsorbed bubbles on the electrode surface not only cover the active sites of Co_3O_4/N-rGO, but also deliver a higher pressure in the electrolyte.[4] As shown in **Fig. S25**, The contact angle of the Co_3O_4/N-rGO-Light electrode (28.9°) is much smaller than that of the Co_3O_4/N-rGO electrode (95.4°), revealing that the photothermal effect can significantly improve the wetting ability of the electrode and in turn reduces the bubble adhesion as well as the size at which bubbles release from the surface.[5] The promotion of wetting ability of the electrode via photothermal effect can be rationalized as follows. The photothermal effect triggers the temperature rise of electrolyte near the surface of electrode due to the heat transfer (**Fig. 3c**). When the temperature increases, the interaction between water molecules weakens, leading to a decrease in the surface tension of water[6]. The value of the contact angle can reflect the wetting ability of the liquid to the solid. The reduced surface tension of water decreases the corresponding contact angle θ based on the Young and Young-Laplace equations[7-9]. To this end, a classical semi-empirical equation considering the Gibbs adsorption isotherm and thermodynamics was proposed to estimate the relationship between contact angle and temperature[10,11]:

$$\cos\theta = 1 + C(T_{C0}\text{-}T)^{a/(b-a)}$$

where T and T_{C0} represent the temperature and critical temperature (i.e. the temperature at which the contact angle drops to 0), C is a constant, and a and b are temperature-invariant constants derived from molecular theory. This semi-empirical equation predicts that the contact angle reduces as the temperature increases[12]. Thus the photothermal effect facilitates to improve the wetting ability of the electrode.

As shown in **Fig. S26**, more O_2 bubbles with smaller size form on the electrode surface with light illumination at the same current density for OER process, indicating that the greatly boosted release speed of O_2 bubbles is realized in the presence of the photothermal effect.

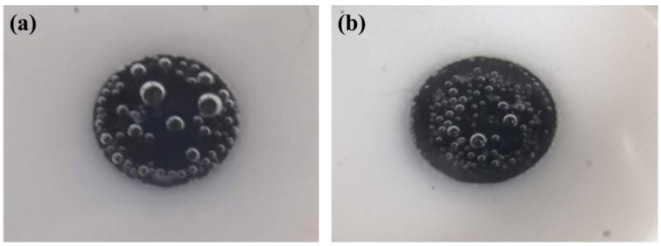

Supplementary Fig. 26 Digital images of the Co_3O_4/N-rGO electrode without (a) and with (b) NIR light irradiation at the same current density for OER process. The NIR light was off at the moment taking the photo of (b) for better clarity.

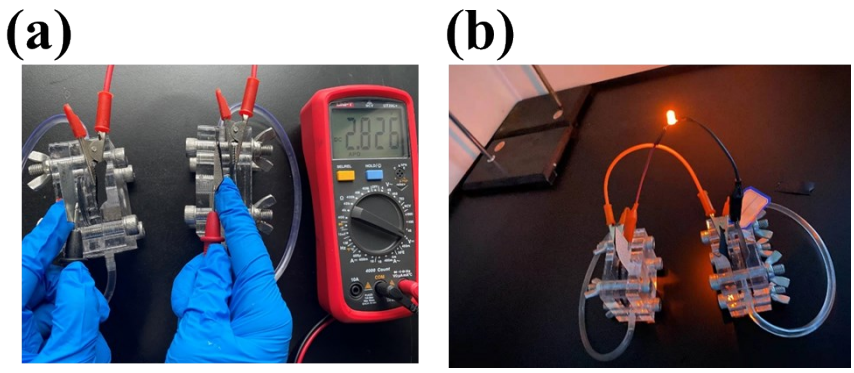

Supplementary Fig. 27 Digital images of (a) open-circuit voltage of two series-connected Co_3O_4/N-rGO-based ZABs and the LED driven by the ZABs.

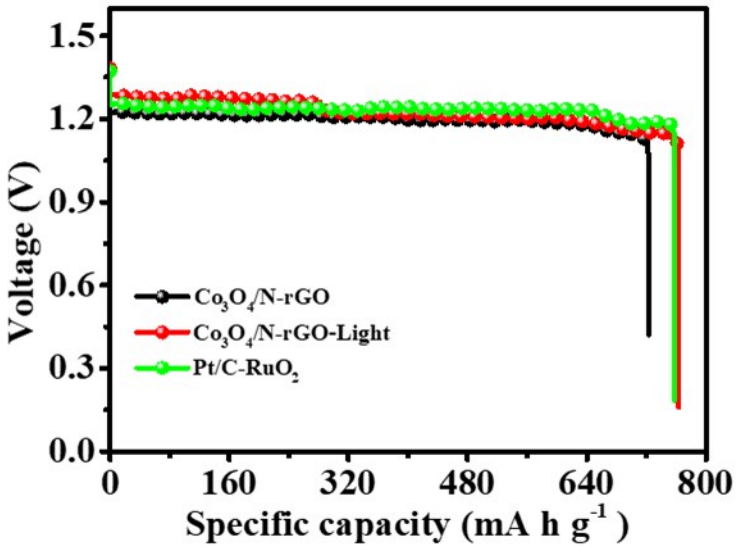

Supplementary Fig. 28 Specific capacities of ZABs at a current density of 10 mA cm^{-2}.

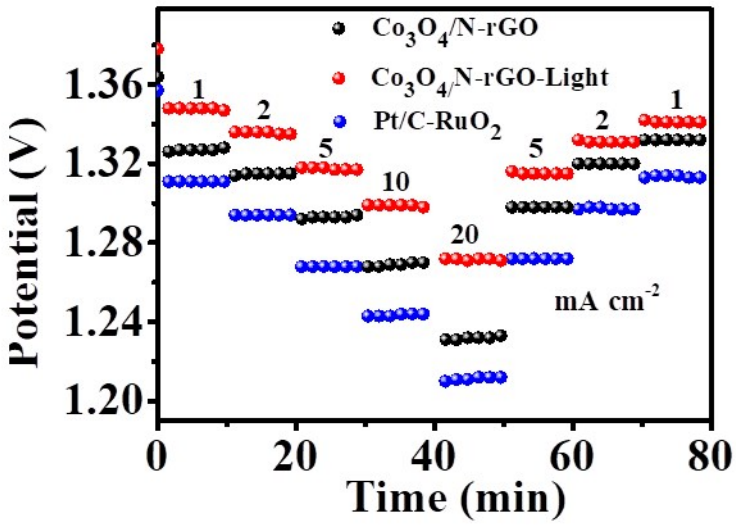

Supplementary Fig. 29 Discharging rate performance of ZABs based on Co_3O_4/N-rGO with and without light, and Pt/C+RuO_2.

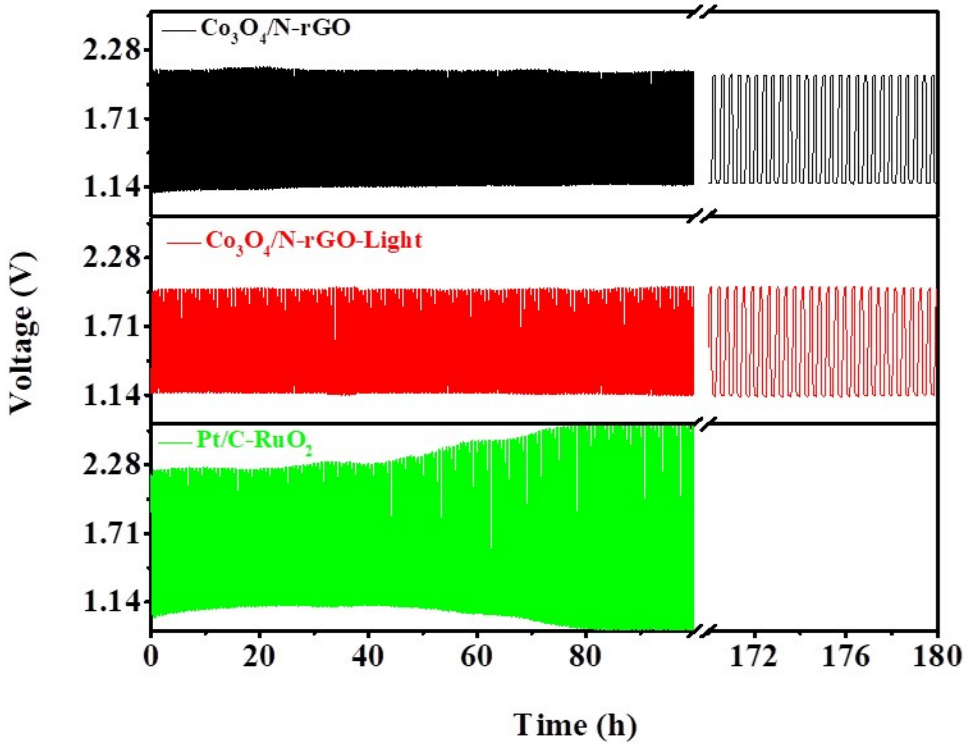

Supplementary Fig. 30 Cycling test of Co_3O_4/N-rGO-based ZABs with and without light and Pt/Ru-based ZAB.

Supplementary Table 1 Comparison of ΔE of the as-synthesized electrocatalysts.

Catalysts	$E_{1/2}$ (V_{RHE})	$E_{j=10}$ (V_{RHE})	ΔE (V)
Co_3O_4/N-rGO-Light	1.485	0.850	0.635
Co_3O_4/N-rGO	1.529	0.835	0.694
Co_3O_4-rGO	1.53	0.804	0.726
Co_3O_4	1.567	0.648	0.919
RuO_2-Pt/C	1.58	0.865	0.715
N-rGO	-	0.814	-

Supplementary Table 2 Comparison of the ORR/OER performance of Co_3O_4/N-rGO with those based on Co_3O_4 electrocatalysts reported in literature.

Catalysts	OER		ORR				ΔE	Ref.
	Electrolytes	η_{10} (mV)	Electrolytes	E_{onset} (V_{RHE})	$E_{1/2}$ (V_{RHE})	J_L (mA cm^{-2})	(V)	
Co_3O_4/N-rGO	1 M KOH	299	0.1 M KOH	0.915	0.835	-5.8	0.694	This work
Co_3O_4/N-rGO-Light	1 M KOH	255		0.934	0.850	-7.1	0.636	
Co_3O_4	0.1 M KOH	380		0.74	0.45	-2	1.16	13
Co_3O_4	1 M KOH	340		0.75	0.67	-3.5	0.9	14
Co_3O_4/N-rGO	1 M KOH	420		0.89	0.82	-3.5	0.83	15
MOF:Co_3O_4@C-MWCNTs	1 M KOH	320		0.89	0.81	-4.5	0.74	16
Co/CNT/MCP	1 M KOH	270		0.94	0.80	−4.8	0.7	17
Meso-Co_3O_4 NPs	0.1 M KOH	411		0.75	0.62	-5.5	1.02	18
Co_3O_4/NHPC	0.1 M KOH	420		0.960	0.835	-6.0	0.815	19
Co_3O_4-NCNT/SS	0.1 M KOH	440		0.95	-	-	-	20
Co_3O_4/N-rGO	0.1 M KOH	490		0.90	0.79	-5.2	0.93	21
PdO-doped Co_3O_4	1 M KOH	350		-	0.83	-5.1	0.76	22
Co_3O_4 NS/ZTC	1 M KOH	380		0.81	0.7	-5.5	0.91	23
Co/Co_3O_4-NG	0.1 M NaOH	437	0.1 M NaOH	0.870	0.617	-4.3	1.05	24

Supplementary Table 3 Comparison of the performance of Co_3O_4/N-rGO-based ZAB with those of ZABs using Co-based electrocatalysts reported in literature.

Catalysts	$E_{1/2}$ (V_{RHE})	$E_{j=10}$ (V_{RHE})	ΔE (V)	Power density (mW cm^{-2})	Ref.
Co_3O_4/N-rGO	0.835	1.529	0.694	175.97	This work
Co_3O_4/N-rGO-Light	0.850	1.485	0.636	299.02	This work
Co-N_x/C NRA	0.870	1.53	0.660	193.2	25
Co/N-codoped	0.827	1.626	0.799	87	26
CoNMC	0.81	1.62	0.81	69.55	27
Co-N-PHCNTs	0.890	1.62	0.730	125.4	28
CoNPC	0.81	1.63	0.82	80	29
Co-BTC	0.79	1.63	0.84	336	30
EA-Co	0.85	1.57	0.72	73	31
Co-N-PCN	0.82	1.61	0.79	-	32
$LaCoO_3$	0.64	1.74	1.10	-	33
Co_3O_4/oCNT	0.75	1.75	1.00	-	34
CoFe/SN/carbon	0.843	1.504	0.661	169	35
Co_3FeN	0.79	1.65	0.86	108	36
CoS-A	0.75	1.62	0.87	-	37
$NiCo_2S_4$ HSs	0.8	1.63	0.83	-	38
f-CoNC/GO	0.82	1.58	0.76	152	39
Co-N,B-CSs	0.83	1.68	0.83	100.4	40
Co-G@POF	0.81	1.66	0.85	241	41
Co_3O_4/NPGC	0.842	1.68	0.838	-	42
$Co_3FeS_{1.5}$(OH)6	0.721	1.588	0.867	113.1	43
CoN_4/NG	0.87	1.61	0.74	28	44
CoPc-GO	0.76	1.6	0.84	-	45
CoS/NSCs	0.876	1.61	0.734	-	46
Co-Ni-S/NSPC	0.82	1.70	0.88	51.6	47
Co_9S_8/C	0.778	1.664	0.886	-	48
Co_3O_4/NBGHSs	0.862	1.70	0.838	330	49
NCNT/$Co_xMn_{1-x}O$	0.84	1.57	0.73	-	50
Ni/NiO/$NiCo_2O_4$/N-CNT	0.74	1.51	0.87	-	51
Co_3O_4/NHPC	0.835	1.65	0.815	80	19

$NiCoO_2$/CNTs	0.67	1.66	0.99	-	52
$NiCoMnO_4$/N-rGO	0.75	1.74	0.99	-	53
CoS_x/Co-NC	0.80	1.54	0.74	103	54
Co_3O_4/N-rmGO	0.8	1.6	0.8	-	55
$NiCo_2S_4$/N/S-rGO	~0.79	1.72	0.93	-	56
Co_9S_8/N-C	0.765	1.565	0.80	-	57
$NiCo_2S_4$/N-CNT	0.80	1.60	0.80	147	58
Co_9S_8/CNT	0.82	1.599	0.779	200	59
Co_9S_8/NSPG-900	0.800	1.573	0.820	-	60
$Fe_{0.5}Co_{0.5}$Ox/NrGO	0.747	1.487	0.740	86	61
MnO@Co–N/C	0.83	1.76	0.93	130.3	62
$NiCo_2O_4$/Co,N-CNTs NCs	0.862	1.569	0.707	173.7	63
Co-POC	0.83	1.7	0.87	78.0	64
CoNi-SAs/NC	0.76	1.57	0.81	-	65
Co-N/HCS	0.86	1.72	0.86	-	66
FeCo(a)-ACM	0.9	1.6	0.7	159.92	67
UNT Co SAs/N-C	0.89	1.61	0.72	-	68
Co-N-C/rGO	0.87	1.72	0.85	-	69
FeCo-NGS	0.84	1.61	1.61	169.43	70
FeCo–N–C	0.896	1.6	0.704	150	71
Co-N-PDEB	0.84	1.92	1.08	-	72
NGM-Co	0.77	1.72	0.95	152	73
$MnCo_2O_{4.5}$	0.7	1.7	1.0	-	74
LT-$Li_{0.5}CoO_2$	0.64	1.57	0.93	-	75
$CuCo_2S_4$NSs	0.70	1.517	0.817	-	76
Co_3O_4/Ni foam	0.75	-	-	35.7	77
Co-NiO	0.79	1.53	0.74	93	78
5%Ni-Co	0.83	1.61	0.78	-	79
N‑GCNT/FeCo	0.92	1.73	0.81	89.3	80
N-CoS_2YSSs	0.81	1.60	0.79	81	81
CoMnON/G	0.807	1.7	0.893	-	82
Na_2CoPO_4F	0.792	1.647	0.855	-	83
N-$NiCo_2O_4$/C	0.81	1.472	0.662	-	84
PtCo-3 NC	0.86	1.616	0.756		85

$MnFe_2O_4/NiCo_2O_4$	0.767	1.574	0.807	-	86
Co/CoO@Co–N-C-800	0.746	1.564	0.818	157	87
Co/CoOx@Co/N-graphene	0.74	-	-	39	88
$Fe_3C/Co(Fe)O_x$@NCNT	0.86	1.58	0.72	231	89
$CuCoO_x$/FeOOH	0.78	1.50	0.72	-	90
Pd@PdO–Co_3O_4	0.727	1.54	0.813	-	91
Pt–$LiCoO_2$	0.81	1.67	0.86	-	92
NiS_2/CoS_2	0.79	1.54	0.75	101	93
In-CoO/CoP FNS	0.81	1.587	0.787	139.4	94
NiO/CoO TINWs	0.803	1.485	0.682	151	95
CoO_xNPs/BNG	0.805	1.525	0.72	-	96
GM-Co-B-N	0.80	1.60	0.80	-	97
Co_3O_4/Ag@NrGO	0.751	1.667	0.916	160	98
Meso - Co_3O_4	0.66	1.62	0.96	-	79
3DCo@N/C	0.812	1.612	0.80	-	99
Co_9S_8/N,S-DLCTs	0.890	1.597	0.707	-	100
S-$Co_{9-x}Fe_xS_8$@rGO	0.84	1.51	0.67	-	101
CoS/NSC	0.84	1.58	0.74	-	102
Co_9S_8@TDC-900	0.78	1.56	0.78	-	103
$Co_{9-x}Ni_xS_8$/NC	0.86	1.65	0.79	75	104
Co–Fe–S@NSRPC	0.80	1.60	0.80	138	105
Co,Mg/S_2@CNTs	0.79	1.59	0.80	268	106
$NiCo_2S_4$/RGO	0.78	1.69	0.91	262.6	107
Co_9S_8/GN	0.8	1.68	0.88	186	108
Co_2P@CoNPG	0.81	1.728	0.92	-	109
Co–N/Co–O/N–C-300	0.80	1.60	0.80	-	110
Co_{1-x}S/N–S–G	0.862	1.601	0.739	-	111
Co_9S_8/NSGg-C_3N_4	0.87	1.65	0.78	-	112
CoS_2(400)/N,S-GO	0.79	1.61	0.82	-	113
$Co_{0.5}Fe_{0.5}$S@N-MC	0.81	1.64	0.83	-	114
Co_9S_8/N,S-CNS	0.8	1.58	0.78		115
Co_3O_4@POF	0.82	1.56	0.74	222.2	116
CoNP/NC/NG-700	0.78	1.62	0.84		117
Co_4N/CNW/CC	0.80	1.54	0.74	174	118

$Ni_{2.25}Co_{0.75}N$/NrGO-3	0.79	1.59	0.80		119
Co / Fe_2Ni_2N @NCNT	0.76	1.63	0.87	-	120
CuCoP-NC-700	0.872	1.567	0.695	116.5	121
$CuCo_2S_4$ NSs@N-CNFs	0.821	1.536	0.715	232	122
FeCo-N/C	0.84	1.61	0.77	-	123
Co@N-CNTF	0.81	1.58	0.77	91	124

Supplementary Table 4 Comparison of the performance of Co_3O_4/N-rGO-based ZAB with those of ZABs using non-Co-based electrocatalysts reported in literature.

Catalysts	$E_{1/2}$ (V_{RHE})	$E_{j=10}$ (V_{RHE})	ΔE (V)	Power density (mW cm^{-2})	Ref.
Co_3O_4/N-rGO	0.835	1.529	0.694	175.97	This work
Co_3O_4/N-rGO-Light	0.850	1.485	0.636	299.02	This work
CFR0.5	0.70	1.49	0.79	-	125
FeNi/N−LCN	0.850	1.570	0.72	162	126
NCNT	0.7	1.62	0.9	-	127
N/C-DT	0.78	1.66	0.88	-	128
$MnFe_2O_4$	0.71	1.82	1.11	-	129
CLSR	0.80	1.72	0.92	50	130
L0.95F	0.38	1.64	1.06	-	131
NPMC	0.85	1.9	-	55	132
$LaCoO_3$	0.64	1.74	1.10	-	33
NB-CN	0.835	1.65	0.815	320	133
mesoporous LSCO	0.72	1.83	1.11	-	134
NiPc/GO	0.65	1.55	0.9	-	45
LTFO/C	0.72	1.77	1.05	-	135
PBSCF-NF	0.69	1.53	0.84	127	136
α-MnO_x/TiC NPs	0.80	1.56	0.76	217.1	137
Ni_3FeN/NRGO	0.70	1.63	0.93	-	138
Fe–N–C/ NiFe-LDH	0.792	1.539	0.747	-	139
BM LSC	0.638	1.761	1.123	-	140
NSCG	0.4	1.67	1.27	5.9	141
FeNC	0.72	1.55	0.83	-	142
CNX	0.66	1.62	0.96	-	143
B,N-carbon	0.84	1.552	0.712	143	144
Fe-NSDC	0.84	1.64	0.80	225.1	145
NPC	0.82	1.62	0.8	-	146
CNT/NCNT	0.71	1.76	1.05	-	147
NGM	0.77	1.67	0.90	-	148
MR20	0.80	1.65	0.85	-	149
NDGs	0.85	1.68	0.83	115.2	150
NCYS	0.81	1.74	0.93	-	151

NSC/IGnP	0.64	1.66	1.02	-	152
CoS-A	0.75	1.62	0.87	-	37
CNTBN$_5$	0.72	1.81	1.09	-	153
NCNT/Co$_x$Mn$_{1-x}$O	0.84	1.57	0.73	-	50
BNPC	0.803	1.78	0.977	-	154
Fe-N$_x$-C	0.91	1.83	0.92	96.4	155
CMO	0.74	1.69	0.95	-	156
LO-NF-NCNTs	0.772	~1.71	0.938	-	157
NiFe-LDH/NrGO	0.75	1.488	0.738	113.1	43
Mn$_{0.5}$(Fe$_{0.3}$Ni$_{0.7}$)$_{0.5}$O$_X$/MWCNTs-O	0.84	1.57	0.73	-	158
LC$_5$N$_5$	0.67	1.63	0.96	-	159
LSCF-6482	0.82	1.65	0.83	-	160
N, S-CN	0.79	1.67	0.88	-	161
N-CCs	0.78	1.69	0.91	-	162
NSC-1100	0.812	1.68	0.868	-	163
NC/GC	0.93	1.57	0.64	-	164
Ni$_{1.9}$FeS$_{1.09}$(OH)$_{4.6}$	0.4	1.496	1.0	-	165
TD-CFs	0.74	1.9	-	-	166
LaNi$_{0.8}$Fe$_{0.2}$O$_3$	0.4	1.49	1.09	-	167
SSC-HG	0.79	1.63	0.84	-	168
NMGF	0.714	1.664	0.95	-	169
LSMF	0.73	1.84	1.11	-	170
N,P-GCNS	0.86	1.57	0.71	-	171
NCHCs	0.8	1.72	0.92	-	172
hSNCNC	0.792	1.639	0.847	-	173
2D-PPCN	0.85	1.5	0.74	-	174
FeCu–N–HC	0.92	1.64	0.72	209.4	35
MnSAC	0.915	1.58	0.665	-	175
P,S-CNS	0.87	1.56	0.69	198	176
S5.84%-LCO	0.704	1.594	0.89	92	177
BFC-FC-0.2	0.90	1.60	0.70	160	178
La$_{0.3}$-5582	0.55	1.56	1.01	-	179
BSCF/NiFe	0.78	0.78	0.785	60	180
20@B-MWCNTs	0.56	1.91	1.35	-	181

HNG-900	0.78	1.69	0.91	68	182
$Ni_{12}P_5$/NCNT	0.77	1.59	0.82	-	183
NiS_x-FeO_y/SCFP	0.78	1.6	0.82	-	184
NCNHP-1-500	0.828	1.54	0.712	-	185
BRCAC8502	0.85	1.68	0.83	53	186
NiFeO@MnO_x	0.805	1.63	0.825	-	187
NCNF	0.82	1.84	1.02	185	188
nNiFe/3D MPC	0.86	1.57	0.71	-	189
Fe-NC SAC	0.88	1.68	0.80	180	190
$Ni_{66}Fe_{34}$-NC	0.85	1.699	0.849	-	191
S,S′-CNT	0.79	1.58	0.79	-	192
$Ni_{0.8}Fe_{0.2}$NSs	0.65	1.46	0.81	-	193
HHPC	0.78	1.58	0.8	260.5	194
1-NH2	0.76	1.45	0.69	-	195
NCO-10	0.73	1.63	0.9	-	196
NHGNs	0.85	1.83	0.98	-	197
FNCO	0.4	1.7		150	198
CNT_BMFePc	0.82	1.71	0.89	-	199
CCO@C	0.87	1.56	0.69	-	200
FePc@N,P-DC	0.903	1.56	0.66	120	201
SHG	0.87	1.56	0.69	-	202
FeN_x-PNC	0.86	1.635	0.775	118	203
PNGF	0.845	1.55	0.705		204
NiSx/NMC	0.89	1.57	0.68	186	205
DG	0.76	1.57	0.81	-	206
S,N-Fe/N/C-CNT	0.85	1.6	0.75	-	25
LFP-5	0.66	1.69	1.03	-	207
Au1Nx	0.76	1.68	0.92	-	208
Ni|MnO/CNF	0.826	1.589	0.763	-	209
G/N-MoS_2	0.716	1.62	0.904	-	210
Ni-N_4/GHSs/Fe-N_4	0.83	1.62	0.79		211-
M-2	0.887	1.584	0.697	124	212
LSM30	0.757	1.83	1.073	181.4	213

References:

(1) Chen, P.; Xu, K.; Zhou, T.; Tong, Y.; Wu, J.; Cheng, H.; Lu, X.; Ding, H.; Wu, C.; Xie, Y. *Angewandte Chemie - International Edition* **2016**, *55*, 2488.

(2) Xue, Y.; Liu, J.; Chen, H.; Wang, R.; Li, D.; Qu, J.; Dai, L. *Angewandte Chemie - International Edition* **2012**, *51*, 12124.

(3) Zhou, L.; Tan, Y.; Ji, D.; Zhu, B.; Zhang, P.; Xu, J.; Gan, Q.; Yu, Z.; Zhu, J. *Science Advances* **2016**, *2*, e1501227.

(4) Lu, Z.; Zhu, W.; Yu, X.; Zhang, H.; Li, Y.; Sun, X.; Wang, X.; Wang, H.; Wang, J.; Luo, J.; Lei, X.; Jiang, L. *Advanced Materials* **2014**, *26*, 2683.

(5) He, B.; Jia, S.; Zhao, M.; Wang, Y.; Chen, T.; Zhao, S.; Li, Z.; Lin, Z.; Zhao, Y.; Liu, X. *Advanced Materials* **2021**, *33*, e2004406.

(6) *Atkins' Physical Chemistry (8th), Oxford University Press* **2009**.

(7) *Fundamentals of Interfacial Engineering, Wiley-VCH* **1997**.

(8) Li, C.; Huang, J.; Li, Z. *Scientific Reports* **2016**, *6*, 26488.

(9) Bakli, C.; P, D. S.; Chakraborty, S. *Nanoscale* **2017**, *9*, 12509.

(10) Song, J.-W.; Fan, L.-W. *Advances in Colloid and Interface Science* **2021**, *288*, 102339.

(11) *Physical Chemistry of Surfaces, Wiley-VCH* **1982**.

(12) Song, J. W.; Zeng, D. L.; Fan, L. W. *J Colloid Interface Sci* **2020**, *561*, 870.

(13) Tomon, C.; Krittayavathananon, A.; Sarawutanukul, S.; Duangdangchote, S.; Phattharasupakun, N.; Homlamai, K.; Sawangphruk, M. *Electrochimica Acta* **2021**, *367*, 137490.

(14) Béjar, J.; Álvarez-Contreras, L.; Ledesma-García, J.; Arjona, N.; Arriaga, L. G. *Journal of Electroanalytical Chemistry* **2019**, *847*, 113190.

(15) Kumar, K.; Canaff, C.; Rousseau, J.; Arrii-Clacens, S.; Napporn, T. W.; Habrioux, A.; Kokoh, K. B. *The Journal of Physical Chemistry C* **2016**, *120*, 7949.

(16) Li, X.; Fang, Y.; Lin, X.; Tian, M.; An, X.; Fu, Y.; Li, R.; Jin, J.; Ma, J. *Journal of Materials Chemistry A* **2015**, *3*, 17392.

(17) Zhou, X.; Liu, X.; Zhang, J.; Zhang, C.; Yoo, S. J.; Kim, J.-G.; Chu, X.; Song, C.; Wang, P.; Zhao, Z.; Li, D.; Zhang, W.; Zheng, W. *Carbon* **2020**, *166*, 284.

(18) Sa, Y. J.; Kwon, K.; Cheon, J. Y.; Kleitz, F.; Joo, S. H. *Journal of Materials Chemistry A* **2013**, *1*, 9992.

(19) Guan, J.; Zhang, Z.; Ji, J.; Dou, M.; Wang, F. *ACS Applied Materials & Interfaces* **2017**, *9*, 30662.

(20) Fu, J.; Hassan, F. M.; Li, J.; Lee, D. U.; Ghannoum, A. R.; Lui, G.; Hoque, M. A.; Chen, Z. *Advanced Materials* **2016**, *28*, 6421.

(21) Li, Y.; Zhong, C.; Liu, J.; Zeng, X.; Qu, S.; Han, X.; Deng, Y.; Hu, W.; Lu, J. *Advanced Materials* **2018**, *30*, 1703657.

(22) Hu, T.; Wang, Y.; Zhang, L.; Tang, T.; Xiao, H.; Chen, W.; Zhao, M.; Jia, J.; Zhu, H. *Applied Catalysis B: Environmental* **2019**, *243*, 175.

(23) Bera, R. K.; Park, H.; Ryoo, R. *Journal of Materials Chemistry A* **2019**, *7*, 9988.

(24) He, B.; Chen, X.; Lu, J.; Yao, S.; Wei, J.; Zhao, Q.; Jing, D.; Huang, X.; Wang, T. *Electroanalysis* **2016**, *28*, 2435.

(25) Chen, P.; Zhou, T.; Xing, L.; Xu, K.; Tong, Y.; Xie, H.; Zhang, L.; Yan, W.; Chu, W.; Wu, C.; Xie, Y. *Angewandte Chemie - International Edition* **2017**, *56*, 610.

(26) Wang, T.; He, Y.; Liu, Y.; Guo, F.; Li, X.; Chen, H.; Li, H.; Lin, Z. *Nano Energy* **2021**, *79*,

105487.

(27) Rong, Z.; Dong, C.; Zhang, S.; Dong, W.; Huang, F. *Nanoscale* **2020**, *12*, 6089.

(28) Guan, Y.; Li, Y.; Luo, S.; Ren, X.; Deng, L.; Sun, L.; Mi, H.; Zhang, P.; Liu, J. *Applied Catalysis B: Environmental* **2019**, *256*, 117871.

(29) Sanetuntikul, J.; Hyun, S.; Ganesan, P.; Shanmugam, S. *Journal of Materials Chemistry A* **2018**, *6*, 24078.

(30) Zhang, X.; Luo, J.; Lin, H.-F.; Tang, P.; Morante, J. R.; Arbiol, J.; Wan, K.; Mao, B.-W.; Liu, L.-M.; Fransaer, J. *Energy Storage Materials* **2019**, *17*, 46.

(31) Zhao, J.; Qin, R.; Liu, R. *Applied Catalysis B: Environmental* **2019**, *256*, 117778.

(32) Tang, Y.; Liu, R.; Liu, S.; Zheng, B.; Lu, Y.; Fu, R.; Wu, D.; Zhang, M.; Rong, M. *Carbon* **2019**, *141*, 704.

(33) Hardin, W. G.; Mefford, J. T.; Slanac, D. A.; Patel, B. B.; Wang, X.; Dai, S.; Zhao, X.; Ruoff, R. S.; Johnston, K. P.; Stevenson, K. J. *Chemistry of Materials* **2014**, *26*, 3368.

(34) Zhao, S.; Rasimick, B.; Mustain, W.; Xu, H. *Applied Catalysis B: Environmental* **2017**, *203*, 138.

(35) Sun, H.; Wang, M.; Zhang, S.; Liu, S.; Shen, X.; Qian, T.; Niu, X.; Xiong, J.; Yan, C. *Advanced Functional Materials* **2020**, *31*, 2006533.

(36) Guo, H.-P.; Gao, X.-W.; Yu, N.-F.; Zheng, Z.; Luo, W.-B.; Wu, C.; Liu, H.-K.; Wang, J.-Z. *Journal of Materials Chemistry A* **2019**, *7*, 26549.

(37) Liu, B.; Qu, S.; Kou, Y.; Liu, Z.; Chen, X.; Wu, Y.; Han, X.; Deng, Y.; Hu, W.; Zhong, C. *ACS Applied Materials & Interfaces* **2018**, *10*, 30433.

(38) Feng, X.; Jiao, Q.; Cui, H.; Yin, M.; Li, Q.; Zhao, Y.; Li, H.; Zhou, W.; Feng, C. *ACS Applied Materials & Interfaces* **2018**, *10*, 29521.

(39) Jia, Y.; Wang, Y.; Zhang, G.; Zhang, C.; Sun, K.; Xiong, X.; Liu, J.; Sun, X. *Journal of Energy Chemistry* **2020**, *49*, 283.

(40) Guo, Y.; Yuan, P.; Zhang, J.; Hu, Y.; Amiinu, I. S.; Wang, X.; Zhou, J.; Xia, H.; Song, Z.; Xu, Q.; Mu, S. *ACS Nano* **2018**, *12*, 1894.

(41) Huang, J.; Zhao, B.; Liu, T.; Mou, J.; Jiang, Z.; Liu, J.; Li, H.; Liu, M. *Advanced Functional Materials* **2019**, *29*, 1902255.

(42) Li, G.; Wang, X.; Fu, J.; Li, J.; Park, M. G.; Zhang, Y.; Lui, G.; Chen, Z. *Angewandte Chemie - International Edition* **2016**, *55*, 4977.

(43) Wang, H. F.; Tang, C.; Wang, B.; Li, B. Q.; Zhang, Q. *Advanced Materials* **2017**, *29*, 1702327

(44) Yang, L.; Shi, L.; Wang, D.; Lv, Y.; Cao, D. *Nano Energy* **2018**, *50*, 691.

(45) Wan, W.; Triana, C. A.; Lan, J.; Li, J.; Allen, C. S.; Zhao, Y.; Iannuzzi, M.; Patzke, G. R. *ACS Nano* **2020**, *14*, 13279.

(46) Xiao, Z.; Xiao, G.; Shi, M.; Zhu, Y. *ACS Applied Materials & Interfaces* **2018**, *10*, 16436.

(47) Fang, W.; Hu, H.; Jiang, T.; Li, G.; Wu, M. *Carbon* **2019**, *146*, 476.

(48) Li, L.; Song, L.; Guo, H.; Xia, W.; Jiang, C.; Gao, B.; Wu, C.; Wang, T.; He, J. *Nanoscale* **2019**, *11*, 901.

(49) Jiang, Z.; Jiang, Z.-J.; Maiyalagan, T.; Manthiram, A. *Journal of Materials Chemistry A* **2016**, *4*, 5877.

(50) Liu, X.; Park, M.; Kim, M. G.; Gupta, S.; Wang, X.; Wu, G.; Cho, J. *Nano Energy* **2016**, *20*, 315.

(51) Ma, N.; Jia, Y.; Yang, X.; She, X.; Zhang, L.; Peng, Z.; Yao, X.; Yang, D. *Journal of Materials Chemistry A* **2016**, *4*, 6376.

(52) Ma, L.; Zhou, H.; Sun, Y.; Xin, S.; Xiao, C.; Kumatani, A.; Matsue, T.; Zhang, P.; Ding, S.; Li, F. *Electrochimica Acta* **2017**, *252*, 338.

(53) Pendashteh, A.; Palma, J.; Anderson, M.; Marcilla, R. *Applied Catalysis B: Environmental* **2017**, *201*, 241.

(54) Lu, Q.; Yu, J.; Zou, X.; Liao, K.; Tan, P.; Zhou, W.; Ni, M.; Shao, Z. *Advanced Functional Materials* **2019**, *29*, 1904481.

(55) Liang, Y.; Li, Y.; Wang, H.; Zhou, J.; Wang, J.; Regier, T.; Dai, H. *Nature materials* **2011**, *10*, 780.

(56) Liu, Q.; Jin, J.; Zhang, J. *ACS Applied Materials & Interfaces* **2013**, *5*, 5002.

(57) Cao, X.; Zheng, X.; Tian, J.; Jin, C.; Ke, K.; Yang, R. *Electrochimica Acta* **2016**, *191*, 776.

(58) Han, X.; Wu, X.; Zhong, C.; Deng, Y.; Zhao, N.; Hu, W. *Nano Energy* **2017**, *31*, 541.

(59) Li, H.; Guo, Z.; Wang, X. *Journal of Materials Chemistry A* **2017**, *5*, 21353.

(60) Ma, X.-X.; Dai, X.-H.; He, X.-Q. *ACS Sustainable Chemistry & Engineering* **2017**, *5*, 9848.

(61) Wei, L.; Karahan, H. E.; Zhai, S.; Liu, H.; Chen, X.; Zhou, Z.; Lei, Y.; Liu, Z.; Chen, Y. *Advanced Materials* **2017**, *29*, 1701410.

(62) Chen, Y.-N.; Guo, Y.; Cui, H.; Xie, Z.; Zhang, X.; Wei, J.; Zhou, Z. *Journal of Materials Chemistry A* **2018**, *6*, 9716.

(63) Li, J.; Lu, S.; Huang, H.; Liu, D.; Zhuang, Z.; Zhong, C. *ACS Sustainable Chemistry & Engineering* **2018**, *6*, 10021.

(64) Li, B. Q.; Zhao, C. X.; Chen, S.; Liu, J. N.; Chen, X.; Song, L.; Zhang, Q. *Advanced Materials* **2019**, *31*, e1900592.

(65) Han, X.; Ling, X.; Yu, D.; Xie, D.; Li, L.; Peng, S.; Zhong, C.; Zhao, N.; Deng, Y.; Hu, W. *Advanced Materials* **2019**, *31*, e1905622.

(66) Cai, S.; Meng, Z.; Tang, H.; Wang, Y.; Tsiakaras, P. *Applied Catalysis B: Environmental* **2017**, *217*, 477.

(67) Chen, C.; Cheng, D.; Liu, S.; Wang, Z.; Hu, M.; Zhou, K. *Energy Storage Materials* **2020**, *24*, 402.

(68) Sun, X.; Sun, S.; Gu, S.; Liang, Z.; Zhang, J.; Yang, Y.; Deng, Z.; Wei, P.; Peng, J.; Xu, Y.; Fang, C.; Li, Q.; Han, J.; Jiang, Z.; Huang, Y. *Nano Energy* **2019**, *61*, 245.

(69) Cai, S.; Wang, R.; Yourey, W. M.; Li, J.; Zhang, H.; Tang, H. *Science Bulletin* **2019**, *64*, 968.

(70) Chen, C.; Li, Y.; Cheng, D.; He, H.; Zhou, K. *ACS Applied Materials & Interfaces* **2020**, *12*, 40415.

(71) Duan, X.; Ren, S.; Pan, N.; Zhang, M.; Zheng, H. *Journal of Materials Chemistry A* **2020**, *8*, 9355.

(72) Kim, K.; Kang, T.; Kim, M.; Kim, J. *Applied Catalysis B: Environmental* **2020**, *275*, 119107.

(73) Tang, C.; Wang, B.; Wang, H. F.; Zhang, Q. *Advanced Materials* **2017**, *29*, 1703185

(74) Bai, Z.; Heng, J.; Zhang, Q.; Yang, L.; Chang, F. *Advanced Energy Materials* **2018**, *8*, 1802390.

(75) Maiyalagan, T.; Jarvis, K. A.; Therese, S.; Ferreira, P. J.; Manthiram, A. *Nature Communications* **2014**, *5*, 3949.

(76) Li, Y.; Yin, J.; An, L.; Lu, M.; Sun, K.; Zhao, Y. Q.; Cheng, F.; Xi, P. *Nanoscale* **2018**, *10*, 6581.

(77) Tan, P.; Chen, B.; Xu, H.; Cai, W.; He, W.; Ni, M. *Applied Catalysis B: Environmental* **2019**, *241*, 104.

(78) Qian, J.; Guo, X.; Wang, T.; Liu, P.; Zhang, H.; Gao, D. *Applied Catalysis B: Environmental* **2019**, *250*, 71.

(79) Song, W.; Ren, Z.; Chen, S. Y.; Meng, Y.; Biswas, S.; Nandi, P.; Elsen, H. A.; Gao, P. X.; Suib, S. L. *ACS Applied Materials & Interfaces* **2016**, *8*, 20802.

(80) Su, C.-Y.; Cheng, H.; Li, W.; Liu, Z.-Q.; Li, N.; Hou, Z.; Bai, F.-Q.; Zhang, H.-X.; Ma, T.-Y. *Advanced Energy Materials* **2017**, *7*, 1602420.

(81) Lu, X. F.; Zhang, S. L.; Shangguan, E.; Zhang, P.; Gao, S.; Lou, X. W. D. *Advanced Science* **2020**, *7*, 2001178.

(82) Li, Y.; Kuttiyiel, K. A.; Wu, L.; Zhu, Y.; Fujita, E.; Adzic, R. R.; Sasaki, K. *ChemSusChem* **2017**, *10*, 68.

(83) Sharma, L.; Gond, R.; Senthilkumar, B.; Roy, A.; Barpanda, P. *ACS Catalysis* **2019**, *10*, 43.

(84) Zhao, C.-X.; Li, B.-Q.; Liu, J.-N.; Huang, J.-Q.; Zhang, Q. *Chinese Chemical Letters* **2019**, *30*, 911.

(85) Hu, S.; Goenaga, G.; Melton, C.; Zawodzinski, T. A.; Mukherjee, D. *Applied Catalysis B: Environmental* **2016**, *182*, 286.

(86) Zhang, Y.-Q.; Li, M.; Hua, B.; Wang, Y.; Sun, Y.-F.; Luo, J.-L. *Applied Catalysis B: Environmental* **2018**, *236*, 413.

(87) Zhang, X.; Liu, R.; Zang, Y.; Liu, G.; Wang, G.; Zhang, Y.; Zhang, H.; Zhao, H. *Chemical Communications* **2016**, *52*, 5946.

(88) Niu, Y.; Huang, X.; Wu, X.; Zhao, L.; Hu, W.; Ming Li, C. *Nanoscale* **2017**, *9*, 10233.

(89) Wang, M.; Qian, T.; Liu, S.; Zhou, J.; Yan, C. *ACS Applied Materials & Interfaces* **2017**, *9*, 21216.

(90) Kuang, M.; Wang, Q.; Ge, H.; Han, P.; Gu, Z.; Al-Enizi, A. M.; Zheng, G. *ACS Energy Letters* **2017**, *2*, 2498.

(91) Li, H.-C.; Zhang, Y.-J.; Hu, X.; Liu, W.-J.; Chen, J.-J.; Yu, H.-Q. *Advanced Energy Materials* **2018**, *8*, 1702734.

(92) Su, C.; Yang, T.; Zhou, W.; Wang, W.; Xu, X.; Shao, Z. *Journal of Materials Chemistry A* **2016**, *4*, 4516.

(93) Cao, Y.; Zheng, X.; Zhang, H.; Zhang, J.; Han, X.; Zhong, C.; Hu, W.; Deng, Y. *Journal of Power Sources* **2019**, *437*, 226893.

(94) Jin, W.; Chen, J.; Liu, B.; Hu, J.; Wu, Z.; Cai, W.; Fu, G. *Small* **2019**, *15*, e1904210.

(95) An, L.; Huang, B.; Zhang, Y.; Wang, R.; Zhang, N.; Dai, T.; Xi, P.; Yan, C. H. *Angewandte Chemie - International Edition* **2019**, *58*, 9459.

(96) Tong, Y.; Chen, P.; Zhou, T.; Xu, K.; Chu, W.; Wu, C.; Xie, Y. *Angewandte Chemie - International Edition* **2017**, *56*, 7121.

(97) Wang, C.; Zhao, Z.; Li, X.; Yan, R.; Wang, J.; Li, A.; Duan, X.; Wang, J.; Liu, Y.; Wang, J. *ACS Applied Materials & Interfaces* **2017**, *9*, 41273.

(98) Wang, Q.; Miao, H.; Sun, S.; Xue, Y.; Liu, Z. *Chemistry – A European Journal* **2018**, *24*, 14816.

(99) Han, M.; Shi, M.; Wang, J.; Zhang, M.; Yan, C.; Jiang, J.; Guo, S.; Sun, Z.; Guo, Z. *Carbon* **2019**, *153*, 575.

(100) Hu, C.; Liu, J.; Wang, J.; She, W.; Xiao, J.; Xi, J.; Bai, Z.; Wang, S. *ACS Applied*

Materials & Interfaces **2018**, *10*, 33124.

(101) Liu, T.; Yang, F.; Cheng, G.; Luo, W. *Small* **2018**, *14*, 1703748

(102) Ren, J.-T.; Yuan, Z.-Y. *ACS Sustainable Chemistry & Engineering* **2019**, *7*, 10121.

(103) Zhao, J.-Y.; Wang, R.; Wang, S.; Lv, Y.-R.; Xu, H.; Zang, S.-Q. *Journal of Materials Chemistry A* **2019**, *7*, 7389.

(104) Cai, Z.; Yamada, I.; Yagi, S. *ACS Applied Materials & Interfaces* **2020**, *12*, 5847.

(105) Fang, W.; Bai, Z.; Yu, X.; Zhang, W.; Wu, M. *Nanoscale* **2020**, *12*, 11746.

(106) Guo, J.; Xu, N.; Wang, Y.; Wang, X.; Huang, H.; Qiao, J. *ACS Applied Materials & Interfaces* **2020**, *12*, 37164.

(107) Liang, Y.; Gong, Q.; Sun, X.; Xu, N.; Gong, P.; Qiao, J. *Electrochimica Acta* **2020**, *342*, 136108.

(108) Sun, X.; Gong, Q.; Liang, Y.; Wu, M.; Xu, N.; Gong, P.; Sun, S.; Qiao, J. *ACS Applied Materials & Interfaces* **2020**, *12*, 38202.

(109) Xuan, J. *International Journal of Electrochemical Science* **2017**, 10471.

(110) Lee, K. J.; Shin, D. Y.; Byeon, A.; Lim, A.; Jo, Y. S.; Begley, A.; Lim, D. H.; Sung, Y. E.; Park, H. S.; Chae, K. H.; Nam, S. W.; Lee, K. Y.; Kim, J. Y. *Nanoscale* **2017**, *9*, 15846.

(111) Qiao, X.; Jin, J.; Fan, H.; Li, Y.; Liao, S. *Journal of Materials Chemistry A* **2017**, *5*, 12354.

(112) Tang, Y.; Jing, F.; Xu, Z.; Zhang, F.; Mai, Y.; Wu, D. *ACS Applied Materials & Interfaces* **2017**, *9*, 12340.

(113) Ganesan, P.; Prabu, M.; Sanetuntikul, J.; Shanmugam, S. *ACS Catalysis* **2015**, *5*, 3625.

(114) Shen, M.; Ruan, C.; Chen, Y.; Jiang, C.; Ai, K.; Lu, L. *ACS Applied Materials & Interfaces* **2015**, *7*, 1207.

(115) Wu, C.; Zhang, Y.; Dong, D.; Xie, H.; Li, J. *Nanoscale* **2017**, *9*, 12432.

(116) Liu, J. N.; Li, B. Q.; Zhao, C. X.; Yu, J.; Zhang, Q. *ChemSusChem* **2020**, *13*, 1529.

(117) Zhong, X.; Jiang, Y.; Chen, X.; Wang, L.; Zhuang, G.; Li, X.; Wang, J.-g. *Journal of Materials Chemistry A* **2016**, *4*, 10575.

(118) Meng, F.; Zhong, H.; Bao, D.; Yan, J.; Zhang, X. *Journal of the American Chemical Society* **2016**, *138*, 10226.

(119) Zhao, M.; Peng, H. J.; Zhang, Z. W.; Li, B. Q.; Chen, X.; Xie, J.; Chen, X.; Wei, J. Y.; Zhang, Q.; Huang, J. Q. *Angewandte Chemie - International Edition* **2019**, *58*, 3779.

(120) Wu, M.; Zhang, G.; Tong, H.; Liu, X.; Du, L.; Chen, N.; Wang, J.; Sun, T.; Regier, T.; Sun, S. *Nano Energy* **2021**, *79*, 105409.

(121) Zhang, H.; Yang, Z.; Wang, X.; Yan, S.; Zhou, T.; Zhang, C.; Telfer, S. G.; Liu, S. *Nanoscale* **2019**, *11*, 17384.

(122) Pan, Z.; Chen, H.; Yang, J.; Ma, Y.; Zhang, Q.; Kou, Z.; Ding, X.; Pang, Y.; Zhang, L.; Gu, Q.; Yan, C.; Wang, J. *Advanced Science* **2019**, *6*, 1900628.

(123) Shui, H.; Jin, T.; Hu, J.; Liu, H. *ChemElectroChem* **2018**, *5*, 1401.

(124) Guo, H.; Feng, Q.; Zhu, J.; Xu, J.; Li, Q.; Liu, S.; Xu, K.; Zhang, C.; Liu, T. *Journal of Materials Chemistry A* **2019**, *7*, 3664.

(125) Jin, X.; Agyeman, D. A.; Kim, S.; Kim, Y. H.; Kim, M. G.; Kang, Y.-M.; Hwang, S.-J. *Nano Energy* **2020**, *67*, 104192.

(126) Li, X.; Liu, Y.; Chen, H.; Yang, M.; Yang, D.; Li, H.; Lin, Z. *Nano Letters* **2021**, *21*, 3098.

(127) Elumeeva, K.; Masa, J.; Sierau, J.; Tietz, F.; Muhler, M.; Schuhmann, W. *Electrochimica*

Acta **2016**, *208*, 25.

(128) Zeng, Z.; Yi, L.; He, J.; Hu, Q.; Liao, Y.; Wang, Y.; Luo, W.; Pan, M. *Journal of Materials Science* **2020**, *55*, 4780.

(129) Si, C.; Zhang, Y.; Zhang, C.; Gao, H.; Ma, W.; Lv, L.; Zhang, Z. *Electrochimica Acta* **2017**, *245*, 829.

(130) Kumar, N.; Kumar, M.; Nagaiah, T. C.; Siruguri, V.; Rayaprol, S.; Yadav, A. K.; Jha, S. N.; Bhattacharyya, D.; Paul, A. K. *ACS Applied Materials & Interfaces* **2020**, *12*, 9190.

(131) Zhu, Y.; Zhou, W.; Yu, J.; Chen, Y.; Liu, M.; Shao, Z. *Chemistry of Materials* **2016**, *28*, 1691.

(132) Zhang, J.; Zhao, Z.; Xia, Z.; Dai, L. *Nature Nanotechnology* **2015**, *10*, 444.

(133) Lu, Z.; Wang, J.; Huang, S.; Hou, Y.; Li, Y.; Zhao, Y.; Mu, S.; Zhang, J.; Zhao, Y. *Nano Energy* **2017**, *42*, 334.

(134) Zhao, Y.; Xu, L.; Mai, L.; Han, C.; An, Q.; Xu, X.; Liu, X.; Zhang, Q. *Proceedings of the National Academy of Sciences* **2012**, *109*, 19569.

(135) Prabu, M.; Ramakrishnan, P.; Ganesan, P.; Manthiram, A.; Shanmugam, S. *Nano Energy* **2015**, *15*, 92.

(136) Bu, Y.; Gwon, O.; Nam, G.; Jang, H.; Kim, S.; Zhong, Q.; Cho, J.; Kim, G. *ACS Nano* **2017**, *11*, 11594.

(137) Song, S.; Li, W.; Deng, Y.-P.; Ruan, Y.; Zhang, Y.; Qin, X.; Chen, Z. *Nano Energy* **2020**, *67*, 104208.

(138) Fan, Y.; Ida, S.; Staykov, A.; Akbay, T.; Hagiwara, H.; Matsuda, J.; Kaneko, K.; Ishihara, T. *Small* **2017**, *13*, 1700099

(139) Dresp, S.; Luo, F.; Schmack, R.; Kühl, S.; Gliech, M.; Strasser, P. *Energy & Environmental Science* **2016**, *9*, 2020.

(140) Oh, M. Y.; Jeon, J. S.; Lee, J. J.; Kim, P.; Nahm, K. S. *RSC Advances* **2015**, *5*, 19190.

(141) Chen, S.; Duan, J.; Zheng, Y.; Chen, X.; Du, X. W.; Jaroniec, M.; Qiao, S.-Z. *Energy Storage Materials* **2015**, *1*, 17.

(142) Mamtani, K.; Jain, D.; Co, A. C.; Ozkan, U. S. *Energy & Fuels* **2017**, *31*, 6541.

(143) Mamtani, K.; Jain, D.; Dogu, D.; Gustin, V.; Gunduz, S.; Co, A. C.; Ozkan, U. S. *Applied Catalysis B: Environmental* **2018**, *220*, 88.

(144) Sun, T.; Wang, J.; Qiu, C.; Ling, X.; Tian, B.; Chen, W.; Su, C. *Advanced Science* **2018**, *5*, 1800036.

(145) Zhang, J.; Zhang, M.; Zeng, Y.; Chen, J.; Qiu, L.; Zhou, H.; Sun, C.; Yu, Y.; Zhu, C.; Zhu, Z. *Small* **2019**, *15*, e1900307.

(146) Ren, J.-T.; Yuan, G.-G.; Weng, C.-C.; Chen, L.; Yuan, Z.-Y. *ChemCatChem* **2018**, *10*, 5297.

(147) Tian, G.-L.; Zhang, Q.; Zhang, B.; Jin, Y.-G.; Huang, J.-Q.; Su, D. S.; Wei, F. *Advanced Functional Materials* **2014**, *24*, 5956.

(148) Tang, C.; Wang, H. F.; Chen, X.; Li, B. Q.; Hou, T. Z.; Zhang, B.; Zhang, Q.; Titirici, M. M.; Wei, F. *Advanced Materials* **2016**, *28*, 6845.

(149) Kang, B.; Jin, X.; Oh, S. M.; Patil, S. B.; Kim, M. G.; Kim, S. H.; Hwang, S.-J. *Applied Catalysis B: Environmental* **2018**, *236*, 107.

(150) Wang, Q.; Ji, Y.; Lei, Y.; Wang, Y.; Wang, Y.; Li, Y.; Wang, S. *ACS Energy Letters* **2018**, *3*, 1183.

(151) Zhou, J.; Wang, M.; Qian, T.; Liu, S.; Cao, X.; Yang, T.; Yang, R.; Yan, C. *Nanotechnology* **2017**, *28*, 365403.

(152) Kim, C.; Gwon, O.; Jeon, I.-Y.; Kim, Y.; Shin, J.; Ju, Y.-W.; Baek, J.-B.; Kim, G. *Journal of Materials Chemistry A* **2016**, *4*, 2122.

(153) Patil, I. M.; Lokanathan, M.; Ganesan, B.; Swami, A.; Kakade, B. *Chemistry* **2017**, *23*, 676.

(154) Qian, Y.; Hu, Z.; Ge, X.; Yang, S.; Peng, Y.; Kang, Z.; Liu, Z.; Lee, J. Y.; Zhao, D. *Carbon* **2017**, *111*, 641.

(155) Han, J.; Meng, X.; Lu, L.; Bian, J.; Li, Z.; Sun, C. *Advanced Functional Materials* **2019**, *29*, 1808872.

(156) Abirami, M.; Hwang, S. M.; Yang, J.; Senthilkumar, S. T.; Kim, J.; Go, W. S.; Senthilkumar, B.; Song, H. K.; Kim, Y. *ACS Applied Materials & Interfaces* **2016**, *8*, 32778.

(157) Wang, Z.; Zhang, F.; Jin, C.; Luo, Y.; Sui, J.; Gong, H.; Yang, R. *Carbon* **2017**, *115*, 261.

(158) Morales, D. M.; Kazakova, M. A.; Dieckhöfer, S.; Selyutin, A. G.; Golubtsov, G. V.; Schuhmann, W.; Masa, J. *Advanced Functional Materials* **2019**, *30*, 1905992.

(159) Wang, H.; Xu, W.; Richins, S.; Liaw, K.; Yan, L.; Zhou, M.; Luo, H. *Electrochimica Acta* **2019**, *296*, 945.

(160) Elumeeva, K.; Masa, J.; Tietz, F.; Yang, F.; Xia, W.; Muhler, M.; Schuhmann, W. *ChemElectroChem* **2016**, *3*, 138.

(161) Qu, K.; Zheng, Y.; Dai, S.; Qiao, S. Z. *Nano Energy* **2016**, *19*, 373.

(162) Huang, J.; Lu, Q.; Ma, X.; Yang, X. *Journal of Materials Chemistry A* **2018**, *6*, 18488.

(163) Su, Y.; Wang, H.; Zhao, J.; Rummeli, M. H.; Gao, Y.; Jiang, Y.-B.; Zhang, L.; Zou, G. *Electrochimica Acta* **2018**, *280*, 258.

(164) Wang, Z.; Lu, Y.; Yan, Y.; Larissa, T. Y. P.; Zhang, X.; Wuu, D.; Zhang, H.; Yang, Y.; Wang, X. *Nano Energy* **2016**, *30*, 368.

(165) Wang, B.; Tang, C.; Wang, H. F.; Li, B. Q.; Cui, X.; Zhang, Q. *Small Methods* **2018**, *2*, 1800055.

(166) Wang, L.; Wang, Y.; Wu, M.; Wei, Z.; Cui, C.; Mao, M.; Zhang, J.; Han, X.; Liu, Q.; Ma, J. *Small* **2018**, *14*, e1800737.

(167) Zhang, D.; Song, Y.; Du, Z.; Wang, L.; Li, Y.; Goodenough, J. B. *Journal of Materials Chemistry A* **2015**, *3*, 9421.

(168) Bu, Y.; Nam, G.; Kim, S.; Choi, K.; Zhong, Q.; Lee, J.; Qin, Y.; Cho, J.; Kim, G. *Small* **2018**, *14*, e1802767.

(169) Wang, H.-F.; Tang, C.; Zhang, Q. *Catalysis Today* **2018**, *301*, 25.

(170) Yuan, R.-h.; He, Y.; He, W.; Ni, M.; Leung, M. K. H. *Applied Energy* **2019**, *251*, 113406.

(171) Li, R.; Wei, Z.; Gou, X. *ACS Catalysis* **2015**, *5*, 4133.

(172) Zheng, X.; Cao, X.; Li, X.; Tian, J.; Jin, C.; Yang, R. *Nanoscale* **2017**, *9*, 1059.

(173) Fan, H.; Wang, Y.; Gao, F.; Yang, L.; Liu, M.; Du, X.; Wang, P.; Yang, L.; Wu, Q.; Wang, X.; Hu, Z. *Journal of Energy Chemistry* **2019**, *34*, 64.

(174) Lei, W.; Deng, Y.-P.; Li, G.; Cano, Z. P.; Wang, X.; Luo, D.; Liu, Y.; Wang, D.; Chen, Z. *ACS Catalysis* **2018**, *8*, 2464.

(175) Shang, H.; Sun, W.; Sui, R.; Pei, J.; Zheng, L.; Dong, J.; Jiang, Z.; Zhou, D.; Zhuang, Z.; Chen, W.; Zhang, J.; Wang, D.; Li, Y. *Nano Letters* **2020**, *20*, 5443.

(176) Shinde, S. S.; Lee, C. H.; Sami, A.; Kim, D. H.; Lee, S. U.; Lee, J. H. *ACS Nano* **2017**, *11*,

347.

(177) Ran, J.; Wang, T.; Zhang, J.; Liu, Y.; Xu, C.; Xi, S.; Gao, D. *Chemistry of Materials* **2020**, *32*, 3439.

(178) Pei, Z.; Yuan, Z.; Wang, C.; Zhao, S.; Fei, J.; Wei, L.; Chen, J.; Wang, C.; Qi, R.; Liu, Z.; Chen, Y. *Angewandte Chemie - International Edition* **2020**, *59*, 4793.

(179) Jung, J. I.; Jeong, H. Y.; Lee, J. S.; Kim, M. G.; Cho, J. *Angewandte Chemie - International Edition* **2014**, *53*, 4582.

(180) Majee, R.; Islam, Q. A.; Bhattacharyya, S. *ACS Applied Materials & Interfaces* **2019**, *11*, 35853.

(181) Cheng, Y.; Tian, Y.; Fan, X.; Liu, J.; Yan, C. *Electrochimica Acta* **2014**, *143*, 291.

(182) Cui, H.; Jiao, M.; Chen, Y.-N.; Guo, Y.; Yang, L.; Xie, Z.; Zhou, Z.; Guo, S. *Small Methods* **2018**, *2*, 1800144.

(183) Lv, J.; Abbas, S. C.; Huang, Y.; Liu, Q.; Wu, M.; Wang, Y.; Dai, L. *Nano Energy* **2018**, *43*, 130.

(184) Cheng, Y.; Li, D.; Shi, L.; Xiang, Z. *Nano Energy* **2018**, *47*, 361.

(185) Liang, Q.; Chen, Z.; Chen, X.; Li, Y. *Journal of Materials Chemistry A* **2019**, *7*, 20310.

(186) Li, Q.; He, T.; Zhang, Y.-Q.; Wu, H.; Liu, J.; Qi, Y.; Lei, Y.; Chen, H.; Sun, Z.; Peng, C.; Yi, L.; Zhang, Y. *ACS Sustainable Chemistry & Engineering* **2019**, *7*, 17039.

(187) Cheng, Y.; Dou, S.; Saunders, M.; Zhang, J.; Pan, J.; Wang, S.; Jiang, S. P. *Journal of Materials Chemistry A* **2016**, *4*, 13881.

(188) Liu, Q.; Wang, Y.; Dai, L.; Yao, J. *Advanced Materials* **2016**, *28*, 3000.

(189) Sun, J.; Lowe, S. E.; Zhang, L.; Wang, Y.; Pang, K.; Wang, Y.; Zhong, Y.; Liu, P.; Zhao, K.; Tang, Z.; Zhao, H. *Angewandte Chemie - International Edition* **2018**, *57*, 16511.

(190) Du, C.; Gao, Y.; Wang, J.; Chen, W. *Journal of Materials Chemistry A* **2020**, *8*, 9981.

(191) Ma, M.; Kumar, A.; Wang, D.; Wang, Y.; Jia, Y.; Zhang, Y.; Zhang, G.; Yan, Z.; Sun, X. *Applied Catalysis B: Environmental* **2020**, *274*, 119091.

(192) El-Sawy, A. M.; Mosa, I. M.; Su, D.; Guild, C. J.; Khalid, S.; Joesten, R.; Rusling, J. F.; Suib, S. L. *Advanced Energy Materials* **2016**, *6*, 1501966.

(193) Yang, R.; An, L.; Zhang, Y.; Zhang, N.; Dai, T.; Xi, P. *ChemCatChem* **2019**, *11*, 6002.

(194) Xiao, X.; Li, X.; Wang, Z.; Yan, G.; Guo, H.; Hu, Q.; Li, L.; Liu, Y.; Wang, J. *Applied Catalysis B: Environmental* **2020**, *265*, 118603.

(195) Li, W.; Xue, S.; Watzele, S.; Hou, S.; Fichtner, J.; Semrau, A. L.; Zhou, L.; Welle, A.; Bandarenka, A. S.; Fischer, R. A. *Angewandte Chemie - International Edition* **2020**, *59*, 5837.

(196) Lee, D. U.; Park, M. G.; Cano, Z. P.; Ahn, W.; Chen, Z. *ChemSusChem* **2018**, *11*, 406.

(197) Zhang, Z.; Cao, T.; Liu, S.; Duan, X.; Liu, L.-M.; Wang, S.; Liu, Y. *Particle & Particle Systems Characterization* **2017**, *34*, 1600207.

(198) Lu, Y.-T.; Chien, Y.-J.; Liu, C.-F.; You, T.-H.; Hu, C.-C. *Journal of Materials Chemistry A* **2017**, *5*, 21016.

(199) Arul, A.; Pak, H.; Moon, K. U.; Christy, M.; Oh, M. Y.; Nahm, K. S. *Applied Catalysis B: Environmental* **2018**, *220*, 488.

(200) Wang, X.; Li, Y.; Jin, T.; Meng, J.; Jiao, L.; Zhu, M.; Chen, J. *Nano Letters* **2017**, *17*, 7989.

(201) Cheng, W.; Yuan, P.; Lv, Z.; Guo, Y.; Qiao, Y.; Xue, X.; Liu, X.; Bai, W.; Wang, K.; Xu, Q.; Zhang, J. *Applied Catalysis B: Environmental* **2020**, *260*, 118198.

(202) Hu, C.; Dai, L. *Advanced Materials* **2017**, *29*, 1604942.

(203) Ma, L.; Chen, S.; Pei, Z.; Huang, Y.; Liang, G.; Mo, F.; Yang, Q.; Su, J.; Gao, Y.; Zapien, J. A.; Zhi, C. *ACS Nano* **2018**, *12*, 1949.

(204) Chai, G.-L.; Qiu, K.; Qiao, M.; Titirici, M.-M.; Shang, C.; Guo, Z. *Energy & Environmental Science* **2017**, *10*, 1186.

(205) Wan, K.; Luo, J.; Zhang, X.; Zhou, C.; Seo, J. W.; Subramanian, P.; Yan, J.-w.; Fransaer, J. *Journal of Materials Chemistry A* **2019**, *7*, 19889.

(206) Jia, Y.; Zhang, L.; Du, A.; Gao, G.; Chen, J.; Yan, X.; Brown, C. L.; Yao, X. *Advanced Materials* **2016**, *28*, 9532.

(207) Li, Z.; Lv, L.; Wang, J.; Ao, X.; Ruan, Y.; Zha, D.; Hong, G.; Wu, Q.; Lan, Y.; Wang, C.; Jiang, J.; Liu, M. *Nano Energy* **2018**, *47*, 199.

(208) Liu, L.; Su, H.; Tang, F.; Zhao, X.; Liu, Q. *Nano Energy* **2018**, *46*, 110.

(209) Ji, D.; Sun, J.; Tian, L.; Chinnappan, A.; Zhang, T.; Jayathilaka, W. A. D. M.; Gosh, R.; Baskar, C.; Zhang, Q.; Ramakrishna, S. *Advanced Functional Materials* **2020**, *30*, 1910568.

(210) Tang, C.; Zhong, L.; Zhang, B.; Wang, H. F.; Zhang, Q. *Advanced Materials* **2018**, *30*, 1705110

(211) Chen, J.; Li, H.; Fan, C.; Meng, Q.; Tang, Y.; Qiu, X.; Fu, G.; Ma, T. *ACS Applied Materials & Interfaces* **2020**, *32*, e2003134.

(212) Ding, J.; Wang, P.; Ji, S.; Wang, H.; Linkov, V.; Wang, R. *Electrochimica Acta* **2019**, *296*, 653.

(213) Yan, S.; Xue, Y.; Li, S.; Shao, G.; Liu, Z. *ACS Applied Materials & Interfaces* **2019**, *11*, 25870.